An Electron Spin Resonance Study of Interactions between Gramicidin A′ and Phosphatidylcholine Bilayers

Mingtao Ge and Jack H. Freed
Baker Laboratory of Chemistry, Cornell University, Ithaca, New York 14853 USA

ABSTRACT The model of microscopic order and macroscopic disorder was used to simulate electron spin resonance spectra of spin-labeled lipids, 5-PC, 10-PC, and 16-PC in multilamellar vesicles of dipalmitoylphosphatidylcholine (DPPC) containing gramicidin A′ (GA) at temperatures above the gel-to-liquid crystal transition of DPPC. The simulations show that at a lower concentration of GA (i.e., molar ratios of DPPC/GA greater than 3), GA has only a slight effect on the acyl chain dynamics. The rotational diffusion rate around the axis parallel to the long hydrocarbon chain remains unchanged or increases slightly, while the rate around the perpendicular axes decreases slightly. These spectra from DPPC/GA mixtures could only be fit successfully with two or more components consistent with the well-known concept of "boundary lipids," that is, the peptide induces structural inhomogeneity in lipid bilayers. However, the spectra were significantly better fit with additional components that exhibit increased local ordering, implying decreased amplitude of rotational motion, rather than immobilized components with sharply a reduced rotational rate. The largest relative effects occur at the end of the acyl chains, where the average local order parameter $\bar{S}_t$ of 16-PC increases from 0.06 for pure lipid to 0.66 for 1:1 DPPC/GA. The inhomogeneity in ordering in DPPC bilayers due to GA decreases with increasing temperature. The hyperfine tensor component A_{zz} increases for 10-PC and 16-PC when GA is incorporated into DPPC bilayers, indicating that water has deeply penetrated into the DPPC bilayers. Simulations of published electron spin resonance spectra of 14-PC in dimyristoylphosphatidylcholine/cytochrome oxidase complexes were also better fit by additional components that were more ordered, rather than immobilized. The average local order parameter in this case is found to increase from 0.11 for pure dimyristoylphosphatidylcholine to 0.61 for a lipid/protein ratio of 50. These spectra and their simulations are similar to the results obtained with 16-PC in the DPPC/GA mixtures. The relevance to studies of lipid-protein interactions for other proteins is briefly discussed.

INTRODUCTION

Lipid-protein interactions have been extensively investigated in both reconstituted and biological membranes by various experimental approaches (Jost and Griffith, 1982; Watts and De Pont, 1986; Selinsky, 1992; Mouritsen, 1986). However, questions such as how the organization and the dynamic properties of the lipid membranes are affected by the integral membrane proteins would benefit from further elucidation. A model suggested by Jost et al. (1973) and supported by Knowles et al. (1979), Watts et al. (1979), Marsh and Watts (1982), Marsh (1989), and Devaux and Seignenret (1985) is based on the idea that the rotational motion of a lipid in the immediate vicinity of the protein (the so-called boundary lipid) is immobilized. This model is based on observations of "two-component-like" electron spin resonance (ESR) spectra from spin-labeled lipids in various protein containing membranes, whereas such two-component-like spectra were not observed in pure lipid membranes. By means of a spectral subtraction method (Marsh, 1989), the broad component in the two-component spectra can be obtained and assigned to the boundary lipid. The rotational correlation time τ_R of the boundary lipid was estimated to be $\geq$50 ns, which is approaching the rigid limit on the ESR time scale (Marsh, 1989). In reconstituted membranes, if the protein/lipid ratio is high, the outer peak separation of the broad component is temperature independent, and this has led to a suggestion that spin-labeled lipid is being trapped between aggregated proteins (Devaux and Seignenret, 1985; Chapman et al., 1977).

In contrast to ESR, an immobilized component was not detected in ^2H nuclear magnetic resonance measurements with reconstituted membrane systems (Seelig et al., 1982; Seelig and Seelig, 1980; Paddy et al., 1981). This discrepancy has been ascribed to the difference in time scale between the ESR and nuclear magnetic resonance (NMR) techniques. The argument is that the exchange rate between the boundary and bulk lipid is slow on the ESR time scale but is fast on the NMR time scale. However, the rate of exchange estimated by ESR and by NMR is very different. For example, for cytochrome *c* oxidase reconstituted systems, it ranges from $\sim 10^7\ s^{-1}$ by ESR (Knowles et al., 1979) to $\sim 10^3\ s^{-1}$ by NMR (Dahlquist et al., 1977; Longmuir et al., 1977; Kang et al., 1979).

In studies by other techniques such as Fourier-transform infrared (FTIR), Mendelsohn et al. (1981) found that the CH_2 symmetric stretching band from the glycophorin/dimyristoylphosphatidylcholine (DMPC) system progressively increased as more protein was added, indicating that the motion of the acyl chain of DMPC increased by the incorporation of glycophorin. Lee et al. (1984) also reported from FTIR measurements that a low concentration of gramicidin A′ (GA) increased the lipid acyl chain motion.

Due to its commercial availability, simple structure, and easy incorporation into lipid bilayers, GA is one of the most

Received for publication 1 June 1993 and in final form 9 August 1993.
Address reprint requests to Dr. Jack H. Freed, Department of Chemistry, B52 Baker Laboratory, Cornell University, Ithaca, NY 14853-1301.

0006-3495/93/11/2106/18 $2.00

extensively studied membrane peptides (Killian, 1992; Langs and Triggle, 1992). It consists of 15 hydrophobic amino acids with the two NH_2 termini linked together by a hydrogen bond. This pentadecapeptide forms a channel dimer that spans the membrane. It has a single-strand $\beta^{6.3}$ structure (Urry, 1971, 1972). Many experimental techniques have been used to study the structure and dynamics of GA and the effect of GA on the organization and dynamics of lipid bilayers (for a recent review, see Killian, 1992).

In an ESR study using oriented multilayers of dipalmitoylphosphatidylcholine (DPPC) containing GA at low water content Tanaka and Freed (1985) showed that GA had only a small effect on the lipid chain motions, and no immobilized component was found. Instead, in the gel phase the effect of the GA was to disorder the nearby lipid so that the region about the GA no longer preserved the macroscopic alignment of the multilayers. In the liquid crystal phase, rapid exchange led to a single average spectrum in which the chain ordering was reduced but motion was only slightly affected. The motional and ordering parameters derived from the ESR spectra from these oriented multilayers were generally found to correctly predict the spectra from vesicle dispersions of the same DPPC/GA/water mixtures. However, as the GA/lipid ratio increased, new peaks appeared in the spectra from the dispersions that were not seen in the oriented multilayers. These new peaks were ascribed to "trapped" lipids. These results indicated that the details of the GA-lipid interaction could be different in vesicles versus oriented multilayers.

The purpose of this present study is to carefully examine the ESR spectra from dispersion samples of DPPC/GA, taking advantage of powerful modern spectral simulation methods (Schneider and Freed, 1989; Crepeau et al., 1987; Shin and Freed, 1989; Kar et al., 1985), in an effort to better intepret the ESR results and to attempt to resolve the discrepancy previously reported between ESR and other techniques. In order to compare with the results from other techniques, multilamellar vesicles with excess water were used in this work.

Of particular relevance to the present work is a ^2H NMR study by Rice and Oldfield (1979) on DMPC that was deuterated at specific sites along the acyl chain. They showed that for DMPC/GA ratios above 15, the acyl chain ordering of DMPC increases with increasing [GA]. Upon further increasing [GA], the chain ordering of DMPC decreases. As [GA] in DMPC bilayers is increased above 40 wt% (DMPC/GA molar ratio ~4), a two-component (powder pattern plus isotropic peak) spectrum was observed. The observation that low [GA] increases the ordering of the lipid chain and high [GA] decreases the ordering was also made by FTIR (Lee et al., 1984; Cortijo et al., 1982), Raman (Short et al., 1987), and solid-state NMR measurements (Cornell et al., 1988). It is important to note that even though the Raman spectrum from a dispersion of DMPC/GA (2:1) shows an acyl chain ordering similar to that in pure DMPC, a comparable spectrum from DMPC/GA cocrystals with the same lipid/GA ratio indicates highly ordered lipid (Short et al., 1987). The picture that emerges from these studies of the effects of GA on lipids is thus a different one from that obtained from previous ESR studies on protein-lipid interactions. That is, there is increased ordering, which yields a decrease in angular amplitude of motion, as opposed to a large decrease in the rate of motion.

We also note that Cornell et al. (1988) found in an x-ray diffraction measurement that high [GA] induced the formation of a nonlamellar phase in DMPC. A ^{31}P NMR study showed a very narrow isotropic peak for diacylphosphatidylcholine dispersions with chain lengths of 14, 16, and 18, when the [GA] is greater than 50 wt% (lipid/GA ~3) (Rajan et al., 1981), which could be consistent with the x-ray result. In a fluorescence measurement, Ho and Stubbs (1992) showed that water penetrates deeply into the protein-lipid interface in large unilamellar 1 palmitoyl-2-oleoyl-*sn*-glycero-phosphatidylcholine (POPC) vesicles containing GA.

In the present study three spin-labeled lipids, 5-PC, 10-PC, and 16-PC, with the doxyl (4′,4-dimethyloxazolidine-*N*-oxyl) radical labeled at C_5, C_{10}, and C_{16} of the acyl chain, respectively, dissolved in multilamellar vesicles of DPPC containing GA, were used to examine the effect of GA on the structure and dynamics of the DPPC bilayers. A wide range of [GA] was used, but we confined our attention to the liquid crystalline phase. ESR data were analyzed using the slow motional ESR spectral simulation programs developed in this laboratory (Schneider and Freed, 1989). Because of the microscopic order of the lipids in the vesicle but the macroscopic disorder of the vesicles in the dispersion, the so-called microscopic order and macroscopic disorder (MOMD) model (Meirovitch et al., 1984) was used.

Once the spectra from these lipid/GA systems are carefully analyzed, we found that we could apply a very similar analysis to previously published ESR spectra for the DMPC/yeast cytochrome oxidase system (Knowles et al., 1979) to demonstrate that they lead to an equivalent interpretation. The relation of this result to other protein/lipid systems is also considered.

MATERIALS AND METHODS

Materials

Gramicidin A′, which is a mixture of gramicidin A, B, and C, was obtained from Sigma Chemical Co. (St. Louis, MO). Spin-labeled lipids 5-PC, 10-PC, and 16-PC are products of Avanti Polar Lipids, Inc. (Birmingham, AL). All materials were used without further purification.

Sample preparation and ESR spectroscopy

Measured amounts of DPPC and GA were dissolved in chloroform and methanol, respectively, and then mixed together. The spin label utilized constituted 0.5 mol% of the total DPPC. After thoroughly mixing the solution, the solvent was evaporated by nitrogen gas flow and was completely removed by pumping the sample overnight. The dried powder sample was inserted into a thin-wall capillary, and excess water was then added. The

sample was heated to 80°C for 20 min to ensure complete hydration of the lipid bilayers. After the sample was cooled to room temperature, the ESR spectrum was taken on a Bruker ER-200 ESR spectrometer equipped with a Varian temperature control unit. The temperature was measured with an accuracy of ±0.5°C by means of a copper-constantan thermocouple inserted at the bottom of the cavity.

Simulations

Information on both ordering and dynamics of the lipid bilayers can be obtained from the simulation of the slow motional ESR spectra (Schneider and Freed, 1989). Here we summarize the important features and the parameters of the simulation.

There are four Cartesian coordinate frames: (*a*) The laboratory frame, (x, y, z), defined by the external magnetic field B_o, with the z-axis fixed along B_o. (*b*) The local director frame (x'', y'', z''), which is associated with the local ordering of the lipid bilayers. It represents the preferred direction of alignment in a local region, that is, in a small fragment of lipid bilayers in a vesicle. The normal to the bilayer for the local fragment is usually taken as the z''-axis, and cylindrical symmetry about this axis is usually assumed. (*c*) The molecular or diffusion frame, (x', y', z'), constitutes the principal axes of rotational diffusion of the acyl chain (or of a segment of the lipid chain, to which the nitroxide radical is attached). In a simplifying assumption, the x', y', z' axes are also taken as the principal molecular axes of alignment of the spin-labeled lipid, and an ordering tensor specifies the extent to which the x', y', z' axes orient relative to the x'', y'', z'' axes (cf. below). (*d*) The magnetic frame (x''', y''', z''') is that frame in which the g tensor of the nitroxide radical is diagonal. By convention, the z'''-axis is defined as parallel to the $2p_z$ orbital of the N atom, and x''' as pointing along the N-O bond. The A tensor principal axes are usually taken to coincide with the x''', y''', z''' axes (Schneider and Freed, 1989). The Euler angles that represent the rotation from the diffusion frame (x', y', z') to the magnetic frame are specified by $\Phi = (0, \phi, 0)$ (Schneider and Freed, 1989).

The values of the g tensor were taken from Tanaka and Freed (1985) and were confirmed by ESR studies at 250 GHz, which provides much better g resolution than conventional ESR at x band (Budil et al., 1989). They are $g_{xx} = 2.0089$, $g_{yy} = 2.0058$, and $g_{zz} = 2.0021$ for all three probes. The hyperfine tensor was determined from rigid limit spectra for the different mixtures of DPPC/GA. The A_{zz} components for the three spin labels are given in Table 1.

The mobility of the lipid chain is characterized by the rotational diffusion constants, $R_\parallel$, $R_\perp$, which are the principal values of an axially symmetric rotational diffusion tensor. In the present model they represent motion parallel and perpendicular, resectively, to the preferred orientation of the long hydrocarbon chain. This is a simple approximation to the complex internal modes of motion of the chain as well as the overall motion (Ferrarini et al., 1989).

Lipid molecules in the bilayers experience ordering potentials, which restrict the amplitudes of the rotational motion. That is, the larger the ordering potential, the smaller will be the range of orientations sampled by the motion. Under the approximations noted above, the ordering potential is usually expressed as an expansion in generalized spherical harmonics $D^L_{MK}(\Omega)$ (Schneider and Freed, 1989):

$$-\frac{U(\Omega)}{kT} = \epsilon^2_0 D^2_{00}(\Omega) + \epsilon^2_2 (D^2_{02}(\Omega) + D^2_{0-2}(\Omega)) + \epsilon^4_0 D^4_{00}(\Omega) + \epsilon^4_2 (D^4_{02}(\Omega) + D^4_{0-2}) + \cdots$$

where $\Omega = (\alpha, \beta, \gamma)$ are the Euler angles between the molecular (x', y', z') frame and the local director (x'', y'', z'') frame. The ϵ^2_0, ϵ^2_2, ϵ^4_0, ϵ^4_2 are dimensionless potential energy coefficients. Also, k is Boltzmann's constant, and T is the temperature. The commonly used order parameter S is defined by

$$S = \langle D^2_{00} \rangle = \langle \tfrac{1}{2}(3\cos^2\beta - 1) \rangle = \frac{\int d\Omega \exp(-U/kT) D^2_{00}}{\int d\Omega \exp(-U/kT)},$$

and another order parameter $S_2 = \langle D^2_{02}(\Omega) + D^2_{0-2}(\Omega) \rangle$ is defined in a similar manner. It represents the deviation from cylindrical symmetry of the molecular alignment relative to the local director.

TABLE 1 Variation of hyperfine tensor component A_{zz} of 5-PC, 10-PC, and 16-PC with the concentration of GA in DPPC dispersions*

	DPPC/GA						
Probe	∞	50	20	12.5	5	3	1
5-PC	34.3	34.4	34.4	34.6	34.4	34.6	34.6
10-PC	33.7	34.1	34.3	34.3	34.4	34.1	34.2
16-PC	33.0	33.5	33.6	33.6	33.7	33.7	33.8

* Unit of A_{zz}: Gauss; estimated errors: ±0.2 G; ∞ = pure DPPC.

The MOMD model

In multilamellar vesicles, the lipid chains orient uniformly within a local bilayer region or fragment, but these fragments are randomly distributed in space (and reorient slowly as the vesicles rotate). This is the macroscopic disorder in the MOMD model. The ESR spectrum calculated with the MOMD model is thus an average of the ESR spectra from all fragments.

When GA is added to a lipid vesicle, we expect a disruption of the local order of the lipids in the GA neighborhood, as has been observed (Tanaka and Freed, 1985) in oriented multilayers. We wish to distinguish two limiting effects. The first would be a reduction of the magnitude of the local order, S, but no change in the preferred direction of alignment (i.e., its local director). The second is that the magnitude of the local order S is not affected, but the orientation of the local director for lipids at or near the GA surface can be partially randomized by the irregular surface of the GA. Both are disordering effects and would appear as such in the ESR spectra from macroscopically aligned samples (Tanaka and Freed, 1985). However, in a MOMD spectrum, after averaging over all orientations, a change in the extent of ordering of each lipid would still affect the spectrum, but a change in its preferred direction of alignment would not.

Given the feature of the spectra we are dealing with, we shall use the term "disorder" to refer to a reduction in order parameter S of any of the lipids, (i.e., an increase in amplitude of the rotational motion), and we ignore any randomization of the local directors, since the latter cannot be observed in spectra obtained from the vesicle dispersions. The term "disorder" will also be applied to an increase in the *gauche* conformation in the lipid chain, as we discuss next. An all-*trans* chain will be considered an ordered one, whereas one with *gauche* conformers (including kinks) will be considered to be disordered. When needed, the former will be distinguished as "motional amplitude disorder," while the latter will be called "kink disorder." We shall refer to a wide distribution in the degree of ordering of the lipids as heterogeneity in the membrane.

Lipid chain conformation and diffusion tilt

Information not only on the dynamics and ordering but also on the chain conformation of the lipid bilayers can be obtained from the simulation of slow motional ESR spectra.

The preferred alignment of the lipid chains parallel to the bilayer normal subjects the internal motion of the lipid chain to some constraints. For example, g^+g^- and g^-g^+ conformations are virtually suppressed by severe steric overlaps even in a free chain (Flory, 1989). Here g^+ and g^- stand for *gauche*$^+$ and *gauche*$^-$, respectively, which are conformations of a C-C bond that are related to the *trans* form by right- and left-handed rotation, respectively, of approximately 120° (Flory, 1989). The single *gauche* and g^+g^+, g^-g^- conformations, which bend the lipid chain away from the bilayer normal, must have relatively small populations, except in the region near the end of the chain (Seelig and Seelig, 1974). This suggests that the lipid chain

is disordered mainly as a consequence of kinks (g^+tg^- or g^-tg^+), as appears to have been confirmed by an FTIR study with phosphatidylcholine dispersions (Casal and McElhancy, 1990), wherein they found that the concentration of kinks is much higher than that of end-*gauche* and double-*gauche* conformers.

As far as the simulations are concerned, two matters must be addressed. First, what is the parameter to characterize a kink conformation? Second, what is the lifetime of a kink structure, and how does it compare with the ESR time scale? The diffusion tilt angle ϕ of a nitroxide radical is a conformation-related parameter. In Fig. 1, a right rotation of a kink around the C_3-C_4 and C_7-C_8 bonds generates 3 conformations, ttg^+tg^-, g^+tg^-tt, and g^-tg^-tt. This leads to the so-called crankshaft motion (Boyer, 1966), among three conformers. A kink can also move up or down by shifting the rotating bonds up or down by two bonds (Peterson and Chan, 1977). The rotating axis of the kink, that is, the z'-axis for the internal motion of the segment C_3-C_8 is parallel to the C_3-C_4 and C_7-C_8 bonds. Since the bond angle C-C-C is 112° (Sheater and Vand, 1956), the $2p_z$-axis of nitrogen in a doxyl moiety attached to a C atom between C_4 and C_7 makes a 34° angle with the rotating axis of the kink (z'-axis), that is, the doxyl nitroxide radical has a $\phi = 34°$ (cf. Fig. 1). This is to be compared with the case of a doxyl radical attached to a chain or chain segment of an all-*trans* conformation, for which the ϕ angle is 0°.

We note that the rate of *gauche-trans* transformations is about 10^{10} s^{-1} (Ferrarini et al., 1989; Sholnick and Helfand, 1980), which corresponds to fast motion on the ESR time scale. Thus ESR would observe a time average of such conformations. But the crankshaft motion and kink diffusion are expected to be slower than that of *gauche-trans* transformations (Ferrarini et al., 1989), which could imply that they are slow on the ESR time scale, as would be the lifetime of a kink structure. As a matter of fact we found that the quality of our simulations was significantly improved by introducing a component with $\phi = 34°$, and such a component, with its characteristic spectral features, can even be resolved in some of the experimental spectra from DPPC/GA mixtures, as will be shown below. It should be noted that the lineshapes for the (MOMD) ESR spectra with $\phi = 0°$ and $\phi = 34°$ are quite different.

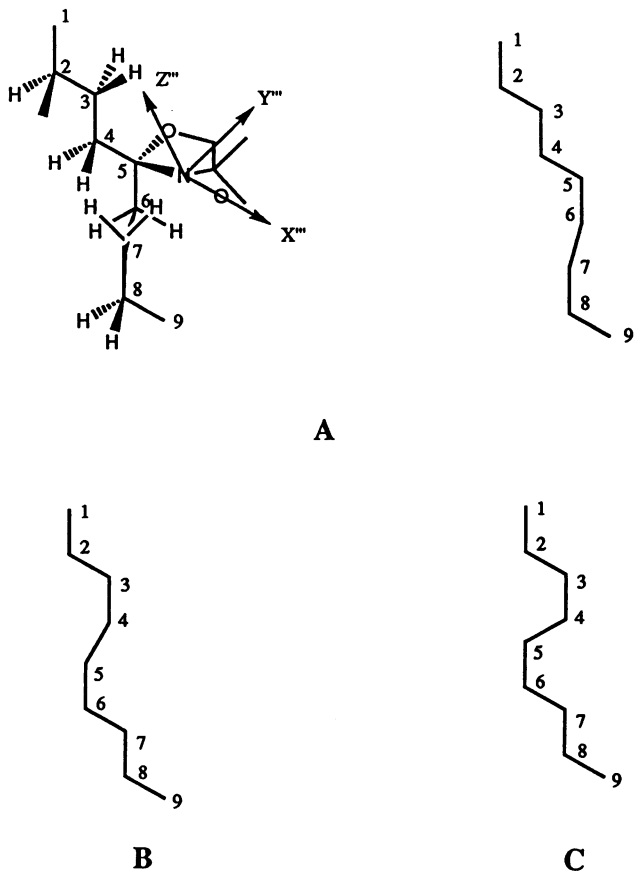

FIGURE 1 Illustration of crank shaft rotation and diffusion tilt angle ϕ. A doxyl nitroxide radical is attached at C_5 in a segment of a lipid acyl chain. The magnetic frame (x''', y''', z''') is shown in the figure; its definition is given in the text. A crank shaft motion of a kink structure generates three conformers (segment C_3–C_8): (*A*) ttg^+tg^-; (*B*) g^+tg^-tt; (*C*) g^-tg^+tt. The rotating axis of the kink, i.e., the z'-axis, is parallel to the C_3–C_4 and C_7–C_8 bonds (they are not colinear). Since the z'''-axis is parallel to the C_4–C_6 line and the bond angle C_4–C_5–C_6 is 112°, the angle between z' and z''', i.e., the difusion tilt angle for the doxyl nitroxide radical, is 34°.

Heterogeneity in lipid/protein mixtures

Heterogeneity in membranes containing protein was predicted in a thermodynamic treatment of protein-lipid interactions by Owicki et al. (1978) and Owicki and McConnell (1979), that is, different lipids may be ordered or disordered to different extents due to the difference in their distances away from the protein, which results in a distribution in order parameter of the lipid chains.

Recently, progress has been made in the analysis of fluorescence lifetime decay in lipid bilayers. Instead of having two discrete exponentials with one dominant, a continuous distribution of lifetimes was found to fit the experimental data much better (Williams and Stubbs, 1988). In particular, Williams et al. (1990) found that the lifetime decay of a fluorophore dissolved in lipid vesicles containing GA is best described by a bimodal Lorentzian distribution with broad distributional width in the major component. Further evidence that membrane peptide or protein will introduce heterogeneity into the bilayer structure can be found from NMR. A dramatic increase in the second moment of the order parameter of DMPC bilayers due to the addition of rhodopsin was observed in a ^2H NMR measurement (Bienvenue et al., 1982). We have observed severe broadening in the two wings of the ESR spectra of spin-labeled lipid in DPPC/GA complexes, which is consistent with the above observations. These observations suggest that a multisite model might lead to good simulations of these ESR spectra. In fact, we could not succeed in obtaining good simulations of many of the experimental spectra with a single-site model, but we did succeed by utilizing models with several sites. For the sake of simplicity, and given our limited resolution, we utilized several discrete components rather than components with continuous distributions in ordering and dynamics. We note that a multisite model was used to interpret the ESR spectra from the DMPC/cytochome oxidase system (Knowles et al., 1979). This included at least three classes of lipid shells, one of which is a boundary shell, but no spectral simulations were performed.

RESULTS AND DISCUSSION

General features of the experimental spectra

ESR spectra of the three spin probes 5-PC, 10-PC, and 16-PC dissolved in multilamellar vesicles of DPPC/GA with a lipid/peptide ratio ranging from 50 to 1 were recorded at temperatures above the gel-to-liquid crystal transition of DPPC. A set of experimental spectra taken at 45°C and their simulations for 16-PC, 5-PC, and 10-PC are depicted in Figs. 2, 3, and 4, respectively. It can be seen that the outermost peak separations of the spectra from all three spin labels increase with [GA]. The 16-PC spectra (Fig. 2) display the characteristic "growing in" of a second component as the [GA] is increased. This is the component usually ascribed to the "immobilized boundary lipid." When Fig. 2 is compared with the ESR results from Tanaka and Freed (1985) (e.g., their Fig. 13), one notes that the spectra are very similar. In particular, the small extra peaks marked by arrows in Fig. 2 are the same

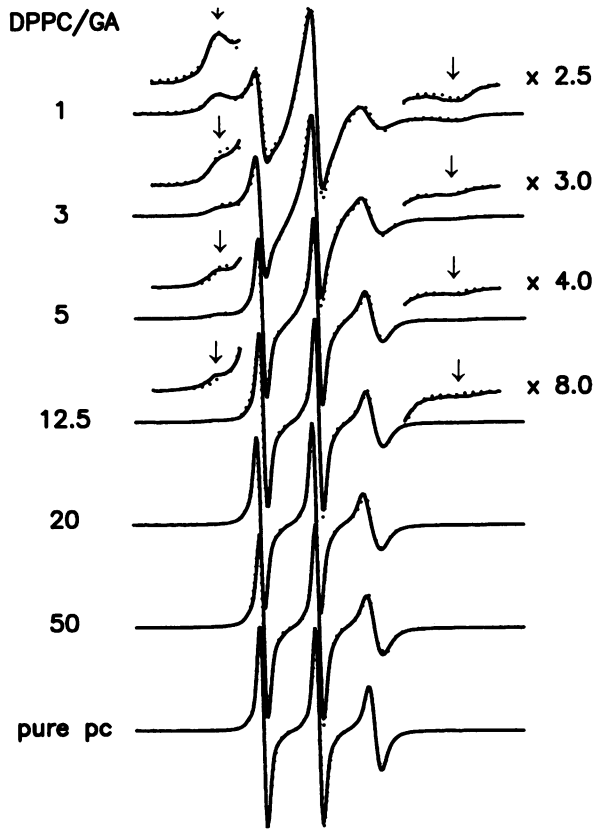

FIGURE 2 Experimental and simulated ESR spectra of 16-PC in multilamellar vesicles of DPPC/GA mixtures with a lipid/peptide ratio ranging from 50 to 1 and with excess water at 45°C. ——, experimental spectra; ·····, simulations.

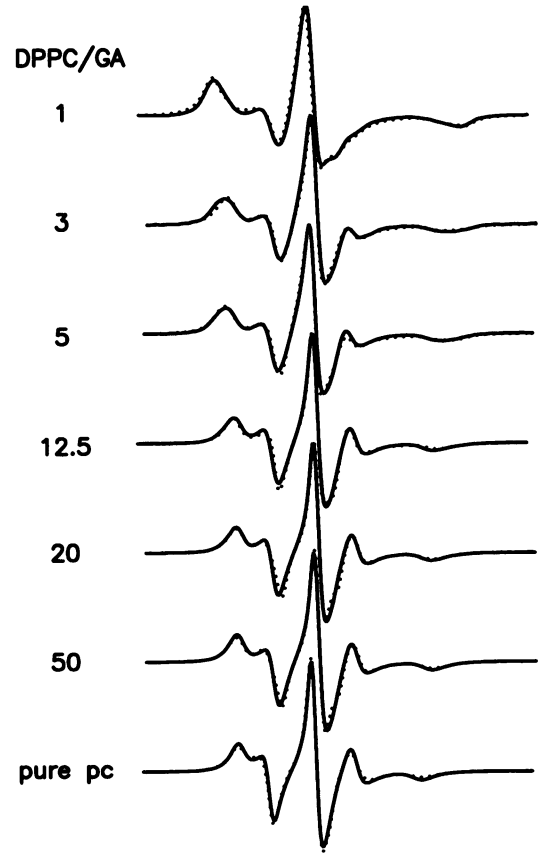

FIGURE 3 Experimental and simulated ESR spectra of 5-PC in multilamellar vesicles of DPPC/GA mixtures with a lipid/peptide ratio ranging from 50 to 1 and with excess water at 45°C. ——, experimental spectra; ·····, simulations.

as those peaks Tanaka and Freed could not fit from the one-site parameters obtained from simulating the spectra from the oriented multilayers. One observes that the spectra from 5-PC (Fig. 3) and 10-PC (Fig. 4) gradually spread out at the two outer wings as more GA is added. The feature of growing in of the broad component as observed for the spectra from 16-PC is absent. A careful examination of Fig. 4 shows an extra "hump" in the spectra of 10-PC (noted by a *vertical arrow*), which would appear to represent an extra component. For doxyl-labeled lipids (for which z' is the ordering axis), an increase in outer peak separation could arise from a decrease in rotational diffusion rate, from an increase in lipid bilayer ordering, or from both. We also note that the line shape change, for all three spin labels, as the DPPC/GA ratio decreases from 3 to 1 is more dramatic as compared to the gradual change of the line shape for DPPC/GA ratios greater than 3.

Simulation of spectra from 16-PC at 45°C

We now describe our approach to the analysis of the ESR line shapes and their changes with [GA]. Our most extensive analyses have been performed on the spectra from 16-PC. This was for two reasons: (*a*) as just noted, its spectral variation with GA is the most dramatic; (*b*) the spectra from pure DPPC containing 16-PC could be very accurately reproduced by a simple model. The first step in simulating the 16-PC spectra was, in fact, to simulate that from pure DPPC by nonlinear least-squares (NLLS) fitting (Crepeau et al., 1987; Shin and Freed, 1989). We consider first the 45°C results. We found it sufficient to vary only $R_\perp$, $R_\parallel$, ϵ^2_0, and ϵ^2_2, and we obtained an excellent fit for values of 5.3×10^8 s^{-1}, 5.6×10^8 s^{-1}, 0.33, and −0.38, respectively, (cf. Table 2). These results imply nearly isotropic rotational motion at the end of the chain. The potential coefficents correspond to order parameters $S = 0.06$ and $S_2 = -0.14$, implying that at the end of the acyl chain, there is a slight preferential alignment of the x'-axis along the director. Note that only two potential parameters were needed in this fit. In general, we found that ESR spectra calculated using the MOMD model are sensitive to $R_\perp$ and ϵ^2_0 and ϵ^2_2 but less sensitive to $R_\parallel$ and to ϵ^4_0 and ϵ^4_2 for $\phi = 0°$. Previous work in this laboratory on oriented samples exhibiting high ordering (not published) have shown that four potential coefficients are required according to a statistical F-test, whereas for the simulation of ESR spectra of low ordering, two potential coefficents are sufficient. So we allowed these four potential coefficients to vary in our fits.

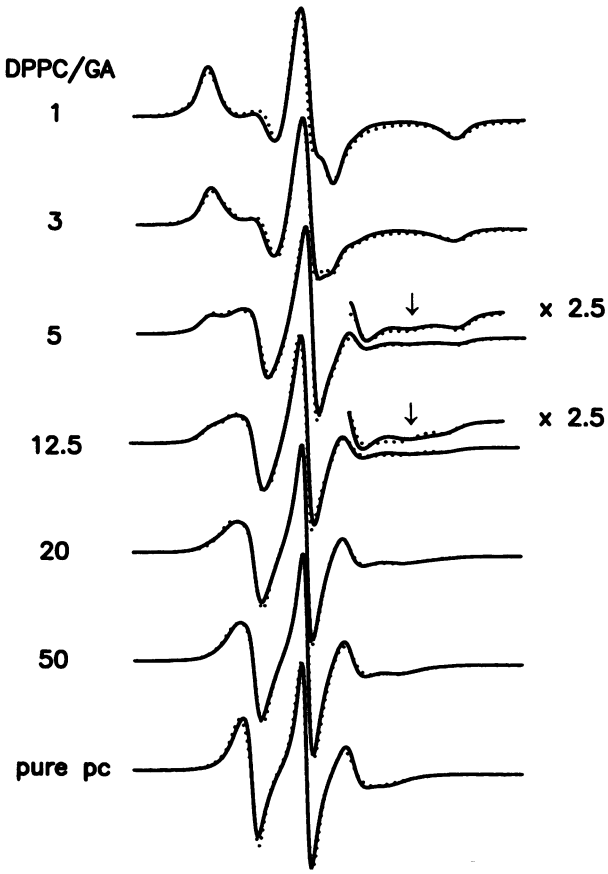

FIGURE 4 Experimental and simulated ESR spectra of 10-PC in multilamellar vesicles of DPPC/GA mixtures with a lipid/peptide ratio ranging from 50 to 1 and with excess water at 45°C. ——, experimental spectra; ·····, simulations. The arrows show an extra component with $\phi = 34°$ (see text and Fig. 10).

TABLE 2 Parameters for the stimulation of ESR spectra of 16-PC in DPPC bilayers at 45°C

$R_\perp$ ($\times 10^8$ s^{-1})	$R_\parallel$ ($\times 10^8$ s^{-1})	ϵ_0^2	ϵ_2^2	ϕ*	S
5.3	5.6	0.33	−0.38	0°	0.06

* ϕ: diffusion tilt angle.

We now summarize how the 16-PC spectra at 45°C were fit as a function of the DPPC/GA ratio. Initially we attempted to use the NLLS fitting for the various compositions. In general, we could not achieve as satisfactory a fit as for pure DPPC in this manner. The smaller the DPPC/GA ratio, the more unsatisfactory was the fit. We expect that this is due to one or more of the simplifying assumptions of the model that is adequate for the pure DPPC but is inadequate to represent how GA affects the lipids. Two possibilities are worth considering. The first is that more than one component is present. This point of view is supported by the results from fluorescence lifetime decay (Williams and Stubbs, 1988) and FTIR (Casal and McElhancy, 1990) (compare above). However, we do note that both fluorescence and FTIR correspond to much shorter time scales than ESR experiments. Even more relevant is the previous ESR study of Tanaka and Freed (1985), which as noted above, appears to confirm the existence of an extra component for the samples with the [GA] greater than 20 mol%. The second possibility would be the inadequacy of the simple diffusional model we use, due to internal versus overall motions (Ferrarini et al., 1989). But the relative freedom of motion of the end chain is probably well approximated by our simple model, and it is satisfactory for pure DPPC. We thus chose to fit the 16-PC spectra as a function of concentration of GA by allowing for two or more components. (We discuss below further aspects of the adequacy of the model for the cases of 10-PC and 5-PC where we believe it is more relevant.)

We did find that the simulations could be improved significantly by admixing components. The most challenging spectrum to fit was that for DPPC/GA = 1. Initially we attempted to fit this spectrum with just two components. The various parameters were adjusted over an extensive range consistent with obtaining the outer peak separation in the experimental spectrum. We could not reproduce all the spectral features in this way. As noted above, previous fluorescence (Williams et al., 1990) and ^{2}H NMR (Bienvenue et al., 1982) as well as our observations lend support to the use of a multisite model, utilizing several discrete components for simplicity. Thus we repeated the procedure utilized for two components with several components until a very good fit was obtained. The variation of parameters was done in a trial-and-error fashion, whereas the final adjustment of relative populations was performed by least squares. We started with a collection of 10 components; by least squares we were able to identify those spectral components that were "sufficiently unique" (i.e., linearly independent from the other components) for a good simulation of the experimental spectrum. In this manner we found that with five components we could obtain a very good fit; (three or four components can reproduce the main features of the experimental spectrum but not all the details). The remaining spectra for DPPC/GA ranging from 3 to 50 were fit with the same five component spectra, wherein only the relative populations were adjusted according to a least-squares procedure. We did find that the number of components needed does decrease with decrease in concentration of GA, that is, from five for a DPPC/GA ratio of 1–3 to two for a DPPC/GA ratio of 50 (cf. Table 4). More significant is the fact that an overall excellent fit is obtained for all of the spectra in this fashion (see Fig. 2).

The most significant way that these components differ from one another is in their ordering. 16-PC in pure DPPC exhibits very low ordering, as we have seen. The additional components have substantially higher ordering, as given in Table 3. As the concentration of GA increases, the admixture of components is such as to substantially increase the average ordering (cf. Table 4). However, the rotational rates, $R_\perp$ and $R_\parallel$, are only slightly changed. That is, $R_\parallel$ increases slightly while $R_\perp$ decreases slightly, except for the two most ordered components, which decrease by factors of about 2 (see Table

TABLE 3 Parameters of the components for the simulation of ESR spectra of 16-PC in DPPC/GA mixtures at 45°C

C	$R_\perp$ ($\times 10^8$ s^{-1})	$R_\parallel$ ($\times 10^8$ s^{-1})	ϵ_0^2	ϵ_2^2	ϵ_0^4	ϵ_2^4	S
1	1.0	10.0	5.2	−1.8	3.0	1.0	0.92
2	2.4	10.0	3.2	−0.5	1.5	0.5	0.78
3	2.9	10.0	2.0	−0.5	1.2	0.3	0.56
4	3.5	8.4	1.2	−0.4	0.5	0.2	0.30
5	4.4	6.7	0.5	−0.4	—	—	0.10

TABLE 4 Populations of the components for the simulation of ESR spectra of 16-PC in DPPC/GA mixtures at 45°C and average order parameters

	Component no.					
DPPC/GA	1	2	3	4	5	$\bar{S}_t$*
1	0.33	0.32	0.11	0.15	0.09	0.66
3	0.05	0.34	0.20	0.20	0.21	0.48
5		0.19	0.36	0.07	0.38	0.41
12.5		0.10		0.20	0.70	0.21
20		0.05		0.17	0.78	0.17
50				0.10	0.90	0.12

* $\bar{S}_t$ = average order parameter of components with all-*trans* conformation.

3). Thus, our analysis implies that the effect of GA is largely to increase the local ordering of the nearby lipid end chains. It does not support the presence of any immobilized species. As will be seen below, this result was also obtained for 5-PC and 10-PC.

TABLE 5 Parameters of components used in the simulation of ESR spectra from 16-PC in DPPC/GA = 1 for models 1 and 2

C†	$R_\perp$ ($\times 10^8$ s^{-1})	$R_\parallel$ ($\times 10^8$ s^{-1})	ϵ_0^2	ϵ_2^2	ϵ_0^4	ϵ_2^4	S	P
Model 1								
1	2.0	5.6						0.18
2	0.8	5.6						0.16
3	0.4	5.6	0.33	−0.38			0.06	0.46
4	0.2	4.0						0.15
5	0.06	1.0						0.05
Model 2								
1			0.8	−0.5	0.5	0.2	0.18	0.15
2			1.2	−0.8	0.6	0.3	0.27	0.45
3	5.3	5.6	2.0	−1.2	0.8	0.4	0.43	0.21
4			4.0	−1.4	2.0	0.8	0.85	0.09
5			6.0	−2.0	3.0	1.2	0.92	0.09

* Model 1, Only motional rates vary; model 2, only ordering varies; model 3, both motional rates and ordering vary; parameters of model 3 are listed in Tables 2, 3, and 4.

† C = component; S = order parameter; P = population.

Comparison of three models

We have attempted to isolate the spectral effects of having components that differ only in their ordering versus components differing only in their motional rates. That is, we addressed the question of whether we could adequetely simulate the spectra by starting with the parameters for the pure DPPC and adding components where only the motional rates were changed (model 1) or only the order parameters were

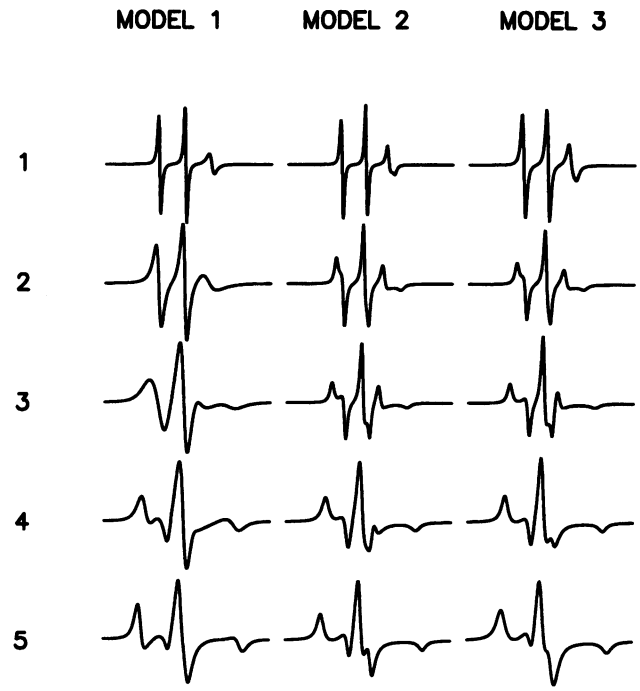

FIGURE 5 The component ESR spectra used in three models. In model 1, only motional rates are varied; in model 2, only ordering is varied; in model 3, both motional rates and ordering are varied. Parameters of these components are listed in Tables 3 and 5.

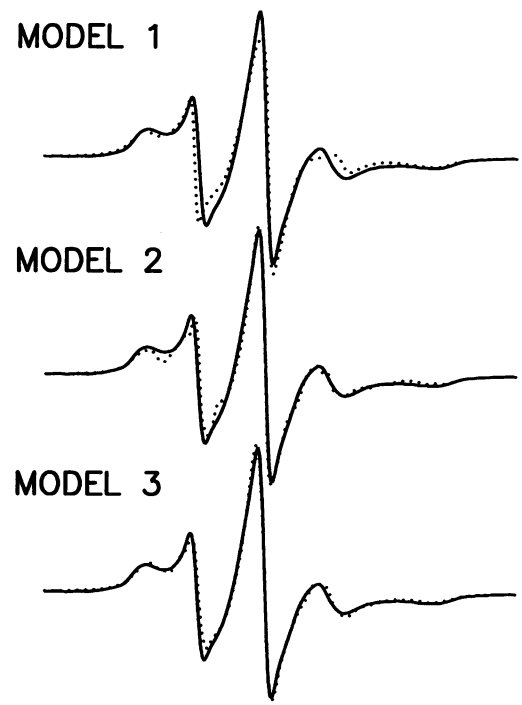

FIGURE 6 Comparison of the simulations of three models. ——, experimental spectrum of 16-PC in a DPPC/GA mixture (1:1) at 45°C; ·····, simulations.

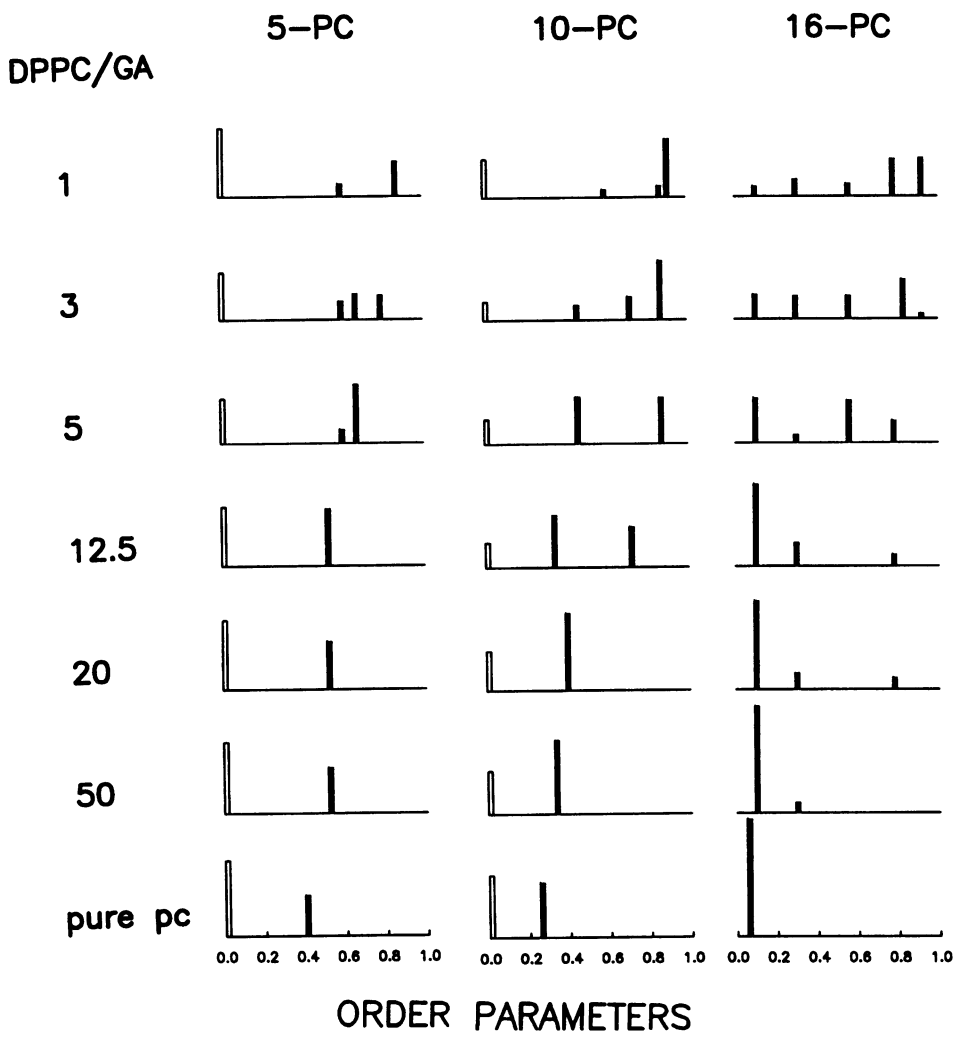

FIGURE 7 Histogram of the distributions in ordering of 5-PC, 10-PC, and 16-PC in DPPC/GA mixtures as a function of DPPC/GA molar ratio at 45°C. Open sticks are relative populations of components with $\phi = 34°$.

changed (model 2). By using the procedure of simulation described above, we started with a set of 10 components in each case, covering an extensive range of motional rates (model 1) or order parameters (model 2) but considered only five at a time in our least-squares estimation of the relative populations. We compared these simulations to the spectrum from a DPPC/GA ratio of 1. The best overall results of the full analysis that yielded the simulations in Fig. 2 (model 3) are given in Tables 3 and 4. The MOMD spectra for each of the five components for each of the three models are shown in Fig. 5. Model 1 requires a very large decrease in $R_\perp$ (by almost two orders of magnitude for the slowest component; cf. Table 5). For model 2, the large variation in S required for the components is comparable to that of model 3. We compare in Fig. 6 the best fitting of models 1, 2, and 3. We find that model 1 yields a simulation that is not entirely satisfactory; model 2 is significantly better, but model 3 is the best of all. Considering that the parameters of the components in model 3 are similar to those of model 2, except for the modest changes in $R_\perp$ and $R_\parallel$, this is not surprising. Obviously, the additional degrees of freedom available to model 3 (i.e., letting $R_\perp$ and $R_\parallel$ vary somewhat) have enabled us to sharpen the quality of the fit. Thus, while the components may differ somewhat in their motional rates, our simulations indicate that the primary effect is the increase of local ordering. This is clearly shown in the histogram plot of the populations of component versus the order parameters (Fig.7), which will be discussed later in more detail.

Simulation of spectra from 16-PC at higher temperatures

Essentially the same procedure was followed for the 16-PC spectra obtained at higher temperatures (60°C, 70°C, and 80°C). At these temperatures we obtained good fits to the spectra for ratios of DPPC/GA more than or equal to 12.5 with just a single component. The high GA concentration spectra at each temperature were again simulated by first fitting the DPPC/GA = 1 spectra with five components by the trial-and-error method described above. These same component spectra were used to fit the remaining compositions at that temperature using a linear least-squares fit to

obtain the relative populations. Excellent fits were obtained in this manner. The distributions as a function of order parameter are illustrated in Fig. 8. As the temperature is increased, the average ordering of the distributions is seen to decrease. A smooth curve has been drawn over the discrete distributions in the spirit of a continuous distribution function, which is suggested by the fluorescence measurement (Williams et al., 1990) (e.g., note the appearance of bimodal distributions). Given the limited resolution of ESR spectra, it is not unreasonable to think of the discrete components that we have used as rough approximations to some continuous distribution. The rotational rates of the lipid chain given by $R_\perp$ and $R_\parallel$ are affected by GA at high temperatures in a manner similar to that at 45°C. The $R_\parallel$ increases by a factor less than or equal to 2, and the $R_\perp$ decreases slightly except for the two most highly ordered components, for which they decrease by factors of 2 to 3.

Simulation of spectra from 5-PC and 10-PC

We now consider the simulation of the spectra from 5-PC and 10-PC. The spectra for the pure DPPC have the feature that they could not be well fit by just one component, especially for 5-PC (cf. Fig. 9). Initially we attempted a NLLS fit for 5-PC using $\phi = 0°$. Our best fit is shown in Fig. 9 *A*, and it is seen to be entirely unsatisfactory. We then let ϕ vary in the NLLS fit and we found that $\phi \approx 34°$, as shown in Fig. 9 *B*. Nevertheless, good agreement was not obtained by any single-component spectrum. Again, one could argue that more than one component is present, perhaps as a result of distinct rotamers that are not rotating sufficiently rapidly around their local bonds. This would be consistent with FTIR studies of DPPC (Mendelsohn et al., 1989) showing the presence of *gauche* rotamers, as well as our discussions (above) showing that a tilt of $\phi = 34°$ is expected in these cases. Alternatively, it may be more appropriate, on the ESR time scale, to have a dynamic interconversion among the various rotamers by the internal modes of motion (Ferrarini et al., 1989). This may be the sounder approach, but no satisfactory theory currently exists to model the combined effects of the already complex, internal plus overall motional dynamics on the ESR line shapes. We therefore took the expedient route of obtaining good fits to the 5-PC spectra in pure DPPC by a superposition of two components, one corresponding to an all-*trans* chain, so that $\phi = 0°$, and the other related to kink structures with $\phi = 34°$. (Given the limited resolution of the MOMD spectra, we suspect that a dynamic average spectrum of such components might also provide good fits.) A third alternative would have been to use the best-fitting single-component simulation that our model provides for. Since we were looking for somewhat subtle changes in the spectrum as a function of the [GA], it was judged to be inadequate to start with a simulation for pure DPPC, which was to serve as the reference. Indeed, the simulation is significantly improved by a superposition of two components, with $\phi = 0°$ and $\phi = 34°$ and relative populations of 35% and 65%, respectively, as is shown in Fig. 9 *C* (cf. Table 6). We did find that for the spectra from DPPC/GA mixtures the use of more than one component was even more important in order to get very good fits. For similar reasons, we also simulated the pure DPPC spectra from 10-PC using two components with $\phi = 0°$ and $\phi = 34°$ (cf. Table 9), although the discrepancies between the best-fitting one-component spectrum and the experimental results were not large.

It should be noted that in our simulations with the MOMD model using $\phi = 34°$, we found that these simulations are

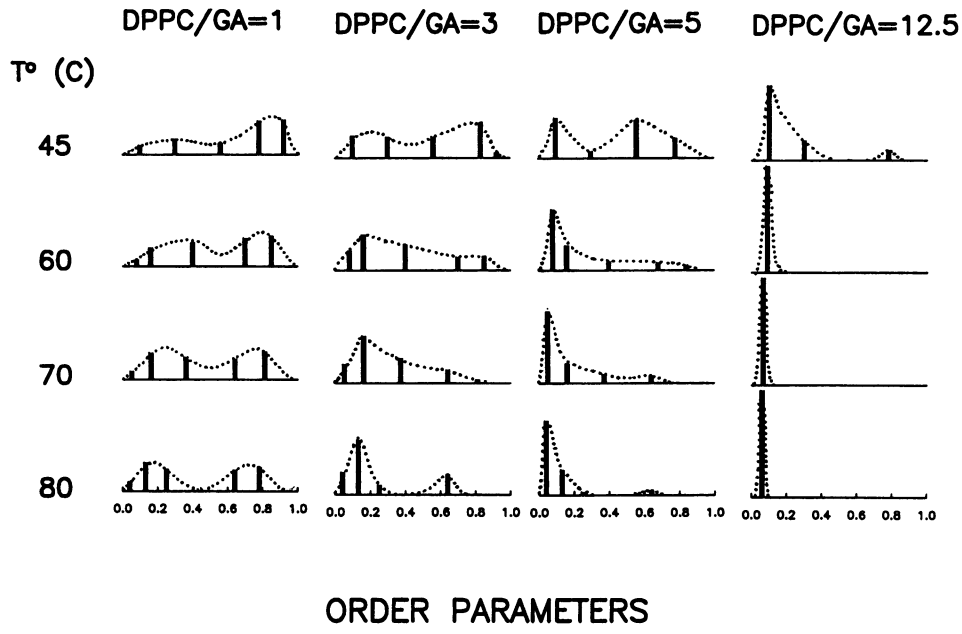

FIGURE 8 Histogram of the distributions in ordering for 16-PC in DPPC/GA mixtures with different molar ratios of lipid/peptide at temperatures of 45°C to 80°C. The dotted envelope illustrates a continuous distribution in ordering.

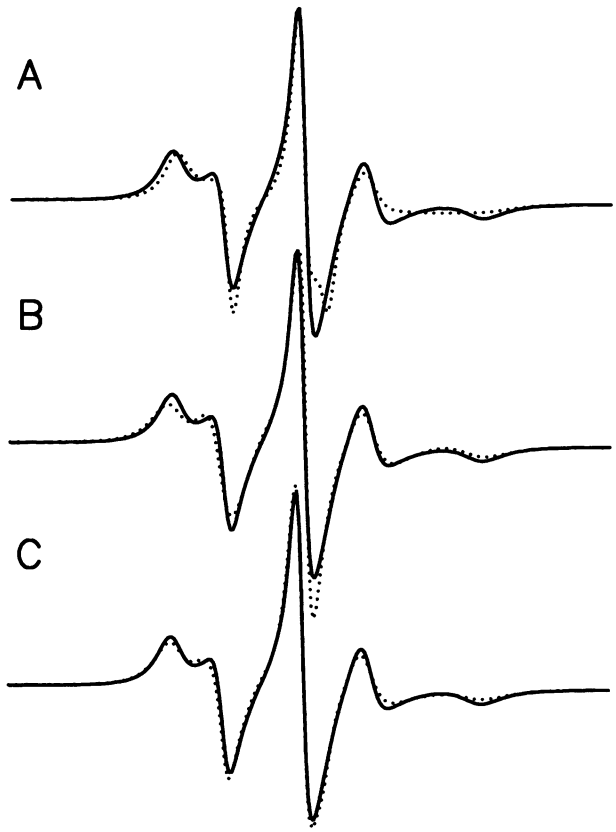

FIGURE 9 (*A* and *B*) experimental and best fit spectra, by NLLS fit, of 5-PC in pure DPPC dispersions at 45°C. ——, experimental spectra; ·····, simulations. (*A*) $\phi = 0°$; (*B*) $\phi = 34°$. (*C*) simulation by a superposition of two components. Parameters of these two components are listed in Table 9.

sensitive to both $R_\perp$ and $R_\parallel$ but are quite insensitive to ordering for $S \leq 0.4$ over the range of $R_\perp$ and $R_\parallel$ values needed. For convenience all components corresponding to $\phi = 34°$ were actually calculated with zero ordering.

The population of the $\phi = 34°$ component at 45°C that we obtained was 0.65 and 0.53, respectively, for 5-PC and 10-PC. These values are about 1.5–2.0 times as high as the fraction of *gauche* rotamers at 48°C at the same position of the DPPC hydrocarbon chain measured by FTIR (Mendelsohn et al., 1989). This may be reasonable, because in our measurement, the population of the component with $\phi = 34°$ using 5-PC (or 10-PC) includes contributions from kink structures which contain the C_5 (or C_{10}) atom, not just the contribution from the C_5 (or C_{10}) atom alone. Note also that we required a $R_\perp$ that was about 5 (for 10-PC) to 13 (for 5-PC) times slower for the $\phi = 34°$ component than for the one with $\phi = 0°$ (see Tables 6 and 9). This would seem to imply that the kink structure suppresses the internal motions that effectively contribute to the $R_\perp$ (Ferrarini et al., 1989). A comparison of Tables 2, 6, and 9 shows that for the $\phi = 0°$ component, $R_\perp$ is about 3 times smaller for 5-PC and 10-PC compared to 16-PC, but $R_\parallel$ is virtually unchanged. The $\phi = 34°$ component is the dominant one for 5-PC (and still the greater one for 10-PC); it would appear that its $R_\perp$ is the more reliable in the event that our use of two components to fit the spectrum is too simplified (compare above).

TABLE 6 Parameters for the simulation of ESR spectra of 5-PC in DPPC bilayers at 45°C

C	$R_\perp$ ($\times 10^8$ s^{-1})	$R_\parallel$ ($\times 10^8$ s^{-1})	ϵ_0^2	ϵ_2^2	ϵ_0^4	ϵ_2^4	ϕ	S	P
1	1.5	5.0	1.5	−0.5	0.8	0.2	0°	0.40	0.35
2	0.12	5.0					34°		0.65

Thus we see that the analysis of the ESR line shapes for 5-PC and 10-PC and their changes with [GA] are somewhat complicated by the assumption of two components for pure DPPC. As in the case of 16-PC, we started with the spectrum for the case of DPPC/GA = 1. We used five components for 5-PC (six for 10-PC) with $\phi = 0°$ and three components for $\phi = 34°$ as we optimized the fit to this spectrum by essentially the same procedure as described above for the 16-PC case. The relative populations were again obtained by linear least-squares (see Tables 8 and 11). In practice, no more than four components were needed to obtain very good fits to any of the spectra (for 5-PC, two were sufficient for DPPC/GA $\geq$ 12.5, three for DPPC/GA = 5, and four for DPPC/GA $\leq$ 3, with a similar result for 10-PC). Thus we find that for DPPC/GA greater than 12.5, no new components are required. However, for DPPC/GA $\leq$ 12.5 there is clear spectral evidence for the appearance of a new component(s). We illustrate this (see Fig. 10) with the three components used for the simulation of the spectrum of 10-PC with a DPPC/GA ratio of 5. One component has a $\phi = 34°$ (component 3); the other two (components 1 and 2) are for 0°. They are displayed above the experimental and simulated spectra. The high field wing of the experimental spectrum is seen to stretch out, forming a plateau in the middle of which there is a hump (indicated by *arrows*). This feature cannot be produced by any components with $\phi = 0°$ but can only be generated by a component with $\phi = 34°$; whereas the outer peak requires the spectrum from one of the $\phi = 0°$ components. To the extent that we have succeeded, in this example, in distinguishing components with $\phi = 0°$ and 34°, the implication is that the lifetime of the kink is comparable to or longer than the ESR time scale.

Effect of GA on the dynamics of DPPC bilayers

A study of Tables 2–4 (for 16-PC) and Tables 6–11 (for 5-PC and 10-PC) leads to the following general observations of the effect of GA on the dynamics of DPPC bilayers: (*a*) For motion with $\phi = 0°$ (i.e., for the motion of an all-*trans* chain or segment), $R_\parallel$ is either not affected or only slightly increased (by a factor of less than 2) over the concentration range of GA studied, while $R_\perp$ decreases slightly (by a factor of less than 4). (*b*) For motion with $\phi = 34°$ (i.e., for motion of involving kinklike structures), $R_\parallel$ increases slightly or remains unchanged at lower [GA] and changes (decreases or increases) slightly at higher [GA] (e.g., for 10-PC, at

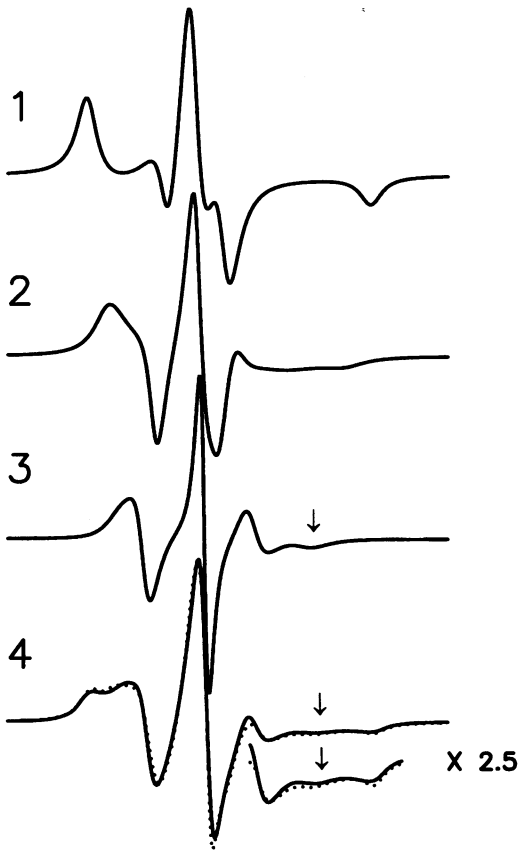

FIGURE 10 Spectra 1, 2, and 3 are three components calculated for the simulation of an experimental spectrum of 10-PC in a DPPC/GA mixture (5:1) at 45°C. Their parameters and relative populations are listed in Tables 10 and 11. The spectra 4 are the experimental spectrum (——) and the simulation (·····), which is generated by admixing the three components (spectra 1, 2, and 3). At the bottom right corner is a part of the experimental and simulated spectra with the intensity magnified by a factor of 2.5. The arrows in the figure show the features in the experimental spectrum that can only be reproduced by component 3 with a $\phi = 34°$ (see text).

DPPC/GA ≥ 5, $R_\parallel$ increases by a factor of less than 3 and at DPPC/GA < 5 decreases by a factor of less than 3), while $R_\perp$ decreases slightly in most cases (e.g., for 10-PC, at DPPC/GA ≥ 5, $R_\perp$ decreases by a factor of less than 2, with similar observations for 5-PC). The significant decrease in $R_\perp$ for $\phi = 34°$ at the highest [GA] (DPPC/GA = 1) would imply that rotation around an axis perpendicular to the long symmetric axis of the kink sequence is highly hindered at high [GA]. The small decrease in $R_\perp$ and small increase in $R_\parallel$ at low [GA] found in our analysis is not inconsistent with an overall effect of slightly increasing lipid chain motion for a dispersion of DMPC/GA (50:1) detected by FTIR (Lee et al., 1984), considering their limited resolution.

TABLE 7 Parameters of components for the simulation of ESR spectra of 5-PC in DPPC/GA mixtures at 45°C

C	$R_\perp$ ($\times 10^8$ s^{-1})	$R_\parallel$ ($\times 10^8$ s^{-1})	ϵ_0^2	ϵ_2^2	ϵ_0^4	ϵ_2^4	ϕ	S
1	0.8	5.0	4.0	−1.6	2.5	0.8	0°	0.87
2	0.9	5.0	3.3	−1.2	1.8	0.7	0°	0.79
3	0.9	5.0	2.5	−1.0	1.5	0.5	0°	0.67
4	1.8	5.0	2.1	−0.8	1.3	0.4	0°	0.60
5	2.0	5.0	1.9	−0.7	1.1	0.3	0°	0.52
6	0.012	1.2					34°	
7	0.030	3.0					34°	
8	0.050	5.0					34°	

Effect of GA on the ordering of DPPC bilayers

The ordering distribution, that is, the relative populations of the components versus the order parameter, for the three spin labels at various [GA] are plotted in Fig. 7 in a histogram form. Due to the uncertainty of the order parameters of the components with $\phi = 34°$, they are all simply taken as zero in the histogram plot (*open columns*). The common features of these plots are that these distributions are broadened by the incorporation of GA, such that the relative populations of the components of high (low) ordering increase (decrease) with increasing [GA], indicative of more locally ordered lipid bilayers but with greater overall inhomogeneity (i.e., a broader distribution in ordering). These features can be quantified by plotting the following three parameters: (*a*) the average order parameter $\bar{S}_t$, (*b*) the population of components with $\phi = 34°$, P_k, and (*c*) the second moment of S, as a function of [GA]. The second moment, ΔS^2, is defined as

$$\Delta S^2 = \sum_i P_i (S_i - \bar{S}_t)^2$$

where P_i is the relative population of the ith component and S_i is the order parameter of the ith component.

As shown in Fig. 11, the $\bar{S}_t$ (calculated by averaging S for the components with $\phi = 0°$ for each spin label at 45°C) increases from 0.06 to 0.66 (16-PC), from 0.26 to 0.86 (10-PC), and from 0.40 to 0.80 (5-PC), respectively, when [GA]

TABLE 8 Populations of the components for the simulation of ESR spectra of 5-PC in DPPC/GA mixtures at 45°C and average order parameters

	Component no.								
DPPC/GA	1	2	3	4	5	6	7	8	$\bar{S}_t$
1	0.30			0.11		0.54	0.05		0.80
3		0.21	0.22	0.16			0.40		0.69
5			0.50	0.12			0.38		0.66
12.5					0.49		0.51		0.52
20					0.41			0.59	0.52
50					0.39			0.61	0.52

TABLE 9 Parameters for the simulation of ESR spectra of 10-PC in DPPC bilayers at 45°C

C	$R_\perp$ ($\times 10^8$ s^{-1})	$R_\parallel$ ($\times 10^8$ s^{-1})	ϵ_0^2	ϵ_2^2	ϵ_0^4	ϵ_2^4	ϕ	S	P
1	1.5	5.0	1.0	−0.3	0.6	0.1	0°	0.26	0.47
2	0.28	4.5					34°		0.53

in DPPC increases from 0 to 50 mol%. The high-order parameter at high concentrations of GA is supported by the previous observation that the cross-sectional area per egg yolk lecithin molecule, measured from a monolayer of lecithin lipid/GA mixture on an air-water interface, is reduced to ~44 Å^2, which is typical of the value for a lecithin molecule with an all-*trans* conformation, when the concentration of GA is between 20 and 40 mol% (Cornell et al., 1978).

P_k is a measure of the disordering of the acyl chain resulting from a kink structure, which is plotted versus [GA] in Fig. 12. In the case of 5-PC, the initial decrease in P_k from 0.65 for pure DPPC to 0.38 for a DPPC/GA ratio of 5, is followed by an increase to 0.59, a value close to that for pure DPPC, as [GA] is further increased to a DPPC/GA ratio of 1. The P_k for 10-PC changes in a similar manner to that for 5-PC.

These results indicate that at very high [GA], concomitant with the ordering effect of GA on the lipid bilayers, a disordering effect also occurs (i.e., an increase in P_k). This is consistent with observations from ^{2}H NMR (Rice and Oldfield, 1979), solid-state NMR (Cornell et al., 1988), Raman (Short et al., 1988), and FTIR (Lee et al., 1984) measurements that low [GA] increases the ordering of the lipid bilayers and high [GA] decreases the ordering of lipid bilayers. We have assumed that all components of 16-PC have $\phi = 0°$. The good agreement between the experimental and simulated spectra does not necessitate the inclusion of any kinks near the 16-PC label. However, this is inconsistent with Rice and Oldfield's observation (1979) that the disordering effect is most prominent at the terminal methyl end of the lipid chain at high concentrations of GA. Due to the greater inhomogeneity in the chain terminal region, as discussed in the next paragraph, and the low resolution of the ESR spectra of 16-PC, we cannot rule out the possibility of a disordering effect at very high concentrations of GA at the terminus of the lipid chain.

TABLE 10 Parameters of the components for the simulation of ESR spectra of 10-PC in DPPC/GA mixtures at 45°C

C	$R_\perp$ ($\times 10^8$ s^{-1})	$R_\parallel$ ($\times 10^8$ s^{-1})	ϵ_0^2	ϵ_2^2	ϵ_0^4	ϵ_2^4	ϕ	S
1	0.4	4.0	4.8	−1.9	3.0	1.1	0°	0.91
2	0.7	5.0	4.0	−1.6	2.5	0.8	0°	0.87
3	0.8	5.0	2.8	−1.0	1.5	0.5	0°	0.72
4	0.9	5.0	2.1	−0.8	1.3	0.4	0°	0.60
5	0.9	5.0	1.7	−0.6	0.9	0.3	0°	0.46
6	1.0	5.0	1.3	−0.5	0.7	0.2	0°	0.34
7	0.04	2.0					34°	
8	0.05	3.5					34°	
9	0.18	12.0					34°	

In Fig. 13, ΔS^2 for the three spin labels is plotted as a function of [GA]. For 5-PC and 10-PC they were calculated from the components of $\phi = 0°$. For 16-PC, the ΔS^2 increases rapidly with [GA] and begins to saturate at a DPPC/GA ratio of 12.5, indicating that a small amount of GA induces significant inhomogeneity in the chain terminal region. From the broader distribution of ordering shown in the histogram plot (cf. Fig. 7) and the associated greater ΔS^2, it is clear that the inhomogeneity in the terminal region is greater than that in the middle or near the headgroup region of the bilayers.

The change of the ordering distribution for 16-PC versus temperature is depicted in Fig. 8. For DPPC/GA $\leq$ 12.5, these distributions have bimodal patterns (Fig. 8). The change of these ordering distributions with temperature is characterized by a shift to lower ordering and a narrowing of the distributions. These two features are displayed in Fig. 14, where $\bar{S}_t$ is plotted versus temperature and in Fig. 15, where ΔS^2 is plotted versus temperature for various [GA].

Water penetrates deeply into DPPC bilayers in DPPC/GA mixtures

Fluorescence measurements have provided evidence that water exists at the peptide-lipid hydrophobic interface of GA in POPC bilayers (Ho and Stubbs, 1992). We found that the hyperfine tensor component, A_{zz}, of 10-PC and 16-PC increases as GA is added to DPPC bilayers. The A_{zz} of 16-PC increases from 33.0 G for pure DPPC to 34.0 G for a DPPC/GA ratio of 1, while for 10-PC, the increase is from 33.7 G to 34.1 G, as shown in Fig. 16. The change in A_{zz} of

TABLE 11 Populations of the components for the simulation of ESR spectra of 10-PC in DPPC/GA mixtures at 45°C and average order parameters

	Component no.									
DPPC/GA	1	2	3	4	5	6	7	8	9	$\bar{S}_t$
1	0.50	0.10		0.07			0.33			0.88
3		0.51	0.20		0.13			0.16		0.77
5		0.39			0.40				0.21	0.66
12.5			0.35			0.44			0.21	0.51
20					0.65				0.35	0.46
50						0.65			0.35	0.34

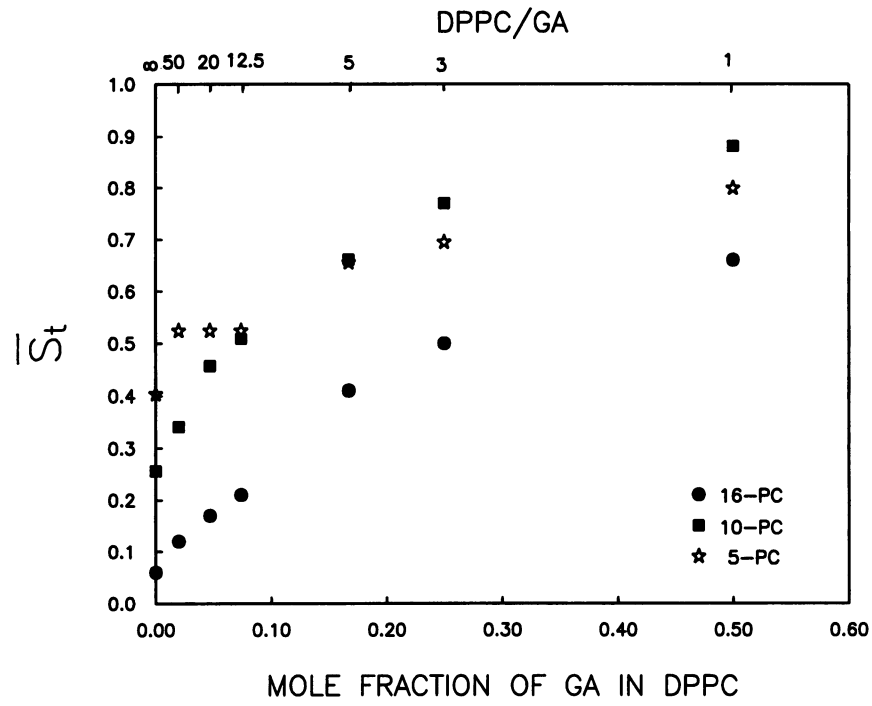

FIGURE 11 Plot of average order parameters $\bar{S}_t$ of 5-PC, 10-PC, and 16-PC in DPPC/GA mixtures as a function of [GA] at 45°C.

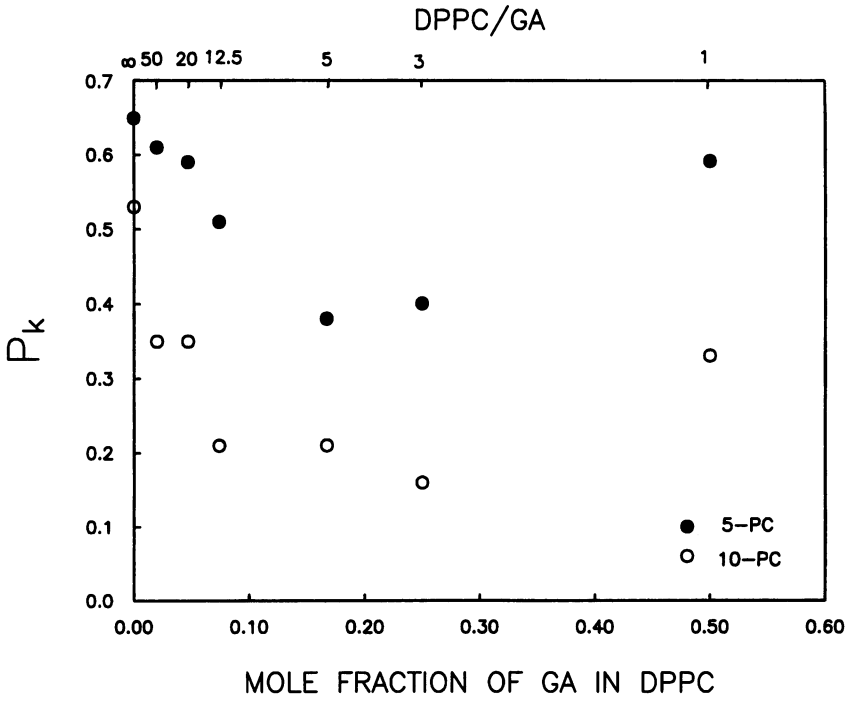

FIGURE 12 Plot of populations of component with $\phi = 34°$, P_k, measured for 5-PC and 10-PC, as a function of [GA] at 45°C.

5-PC is too small to be accurately measured. This is consistent with water having penetrated deeply into the DPPC bilayers (Griffith et al., 1974). Note that in a spin label study of *Halobacterium cutirubrum* cell vesicles, Esser and Lanyi (1973) found that the polarity around the doxyl group of spin-labeled fatty acids in the cell envelope membrane is considerably higher than in the extracted lipid dispersions, indicating that more water has penetrated into the cell envelope membrane than in the lipid. It might be a general rule that membrane proteins and peptides increase the water penetration into lipid bilayers.

The water penetration into lipid bilayers caused by GA may be correlated with the Raman scattering measurements of Short et al. (1987). They found that all dispersion samples of DMPC/GA with excess water are first ordered and then disordered as [GA] increases. However, for DMPC/GA crys-

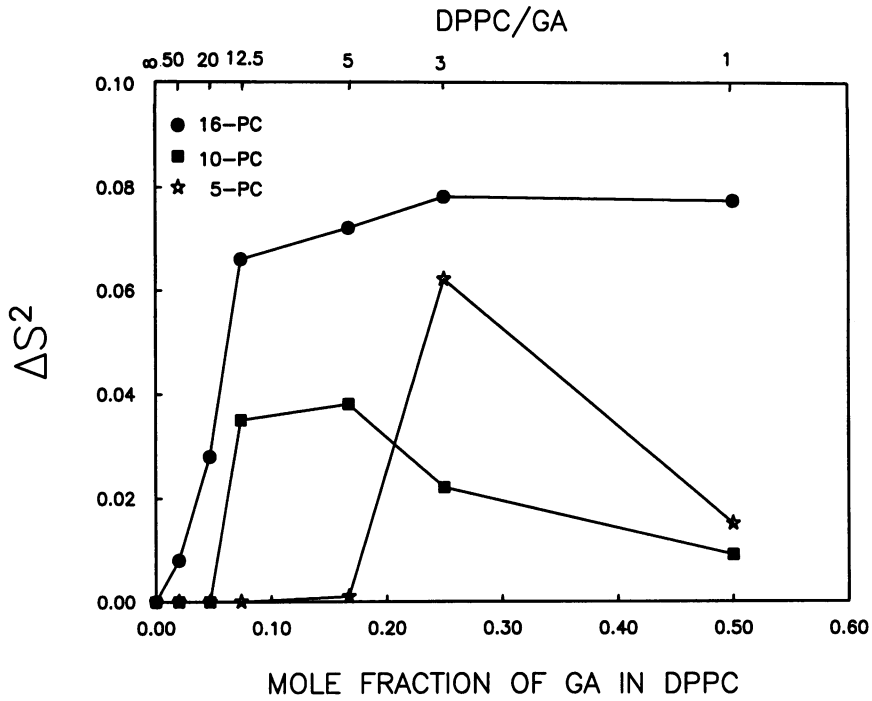

FIGURE 13 Plot of second moment of order parameters, ΔS^2, of 5-PC, 10-PC, and 16-PC as a function of [GA] at 45°C.

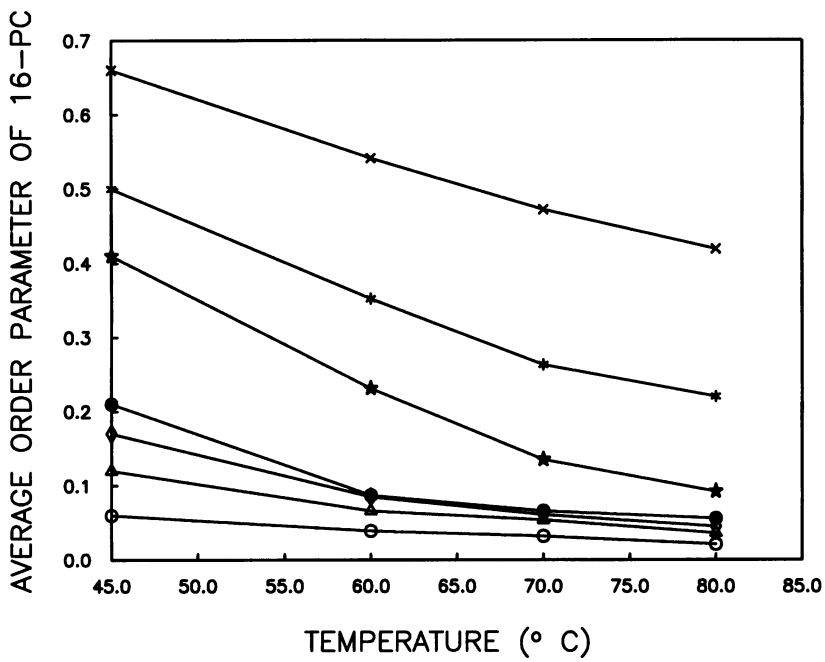

FIGURE 14 Plot of average order parameters of 16-PC, $\bar{S}^2$, as a function of temperature at different [GA]. DPPC/GA: ×, 1; *, 3; ★, 5; ●, 12.5; ◇, 20; △, 50; ○, pure DPPC.

tals (containing no water), no disordering effect was found, even at very high [GA]. These results suggest that the water entering the lipid/GA interface might be responsible for the disordering effect of high [GA]; thus the lipids around the GA molecules, that is, the "boundary lipid," are most likely to be disordered. That is the same suggestion made by Rice and Oldfield (1979). The results of our simulations of spectra from 5-PC and 10-PC (Fig. 7) show that the disordering effect of high [GA] is more precisely an increase in P_k, the concentration of kink structures, that is, kink disorder. The end chains monitored by 16-PC do continue to show an increase in order parameter, implying reduced "motional amplitude disorder."

Relevance to lipid-protein interactions

The ESR spectra from Knowles et al. (1979) of 14-PC in a DMPC/yeast cytochrome oxidase complex showed trends very similar to those of 16-PC in the DPPC/GA system described above, and they were simulated in the same way.

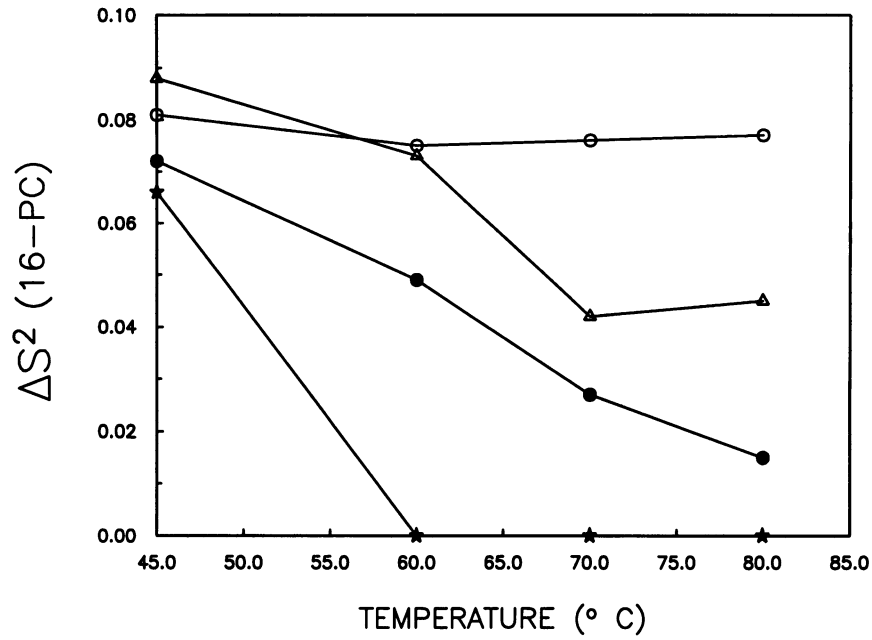

FIGURE 15 Plot of second moment of order parameter, ΔS^2, of 16-PC as a function of temperature at different [GA]. DPPC/GA: ○, 1; △, 3; ●, 5; ★, 12.5.

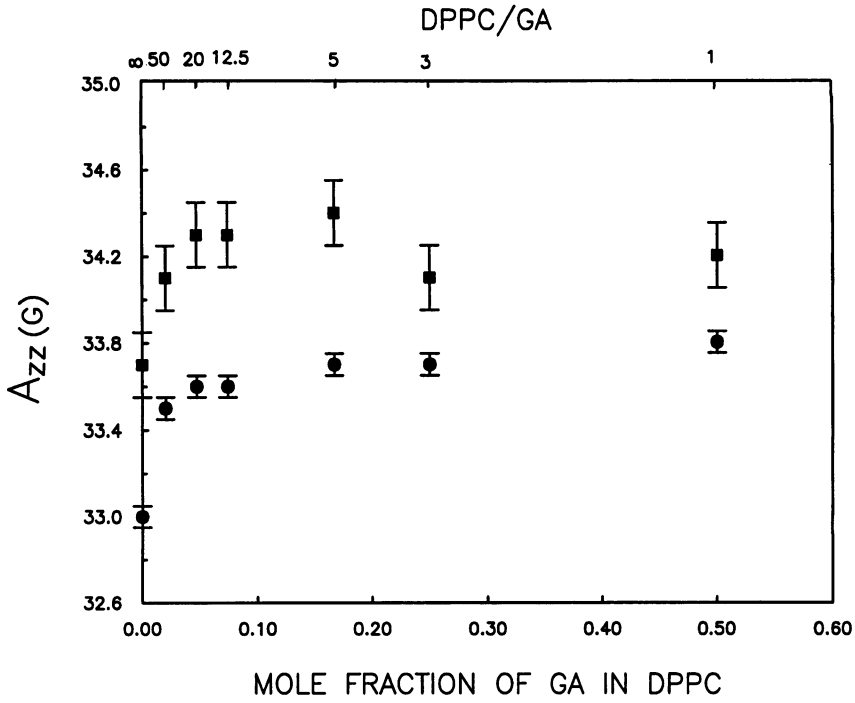

FIGURE 16 Plot of A_{zz} for 5-PC and 10-PC as a function of [GA]. ■, 10-PC; ●, 5-PC.

The digitized experimental spectra and simulations are shown in Fig. 17, and the agreement between them is very good. The parameters obtained from the simulation are listed in Tables 12 and 13. As shown by these parameters, the effects of yeast cytochrome oxidase on the ordering and dynamics of DMPC bilayers are qualitatively much the same as that of GA on the DPPC bilayers that we have found above. The average order parameter increases with the concentration of cytochrome oxidase from 0.11 for pure DMPC to 0.61 for a lipid/protein ratio of 50. Meanwhile, $R_\perp$ decreases and $R_\parallel$ increases by a factor of only 2. Just as in our analysis of the spectra from DPPC/GA mixtures, we could achieve good agreement with a model of increased ordering rather than a model of "immobilized lipid." These results are consistent with that from a fluoresence study of the DMPC/cytochrome oxidase system by Kinosita et al. (1981), who found that the wobbling diffusion constant of fluorescence probe 1,6-diphenyl-1,3,5-hexatriene is not much different in the presence of the protein from that in pure lipid, whereas the cone angle of the wobbling diffusion of the probe decreases in protein-containing vesicles.

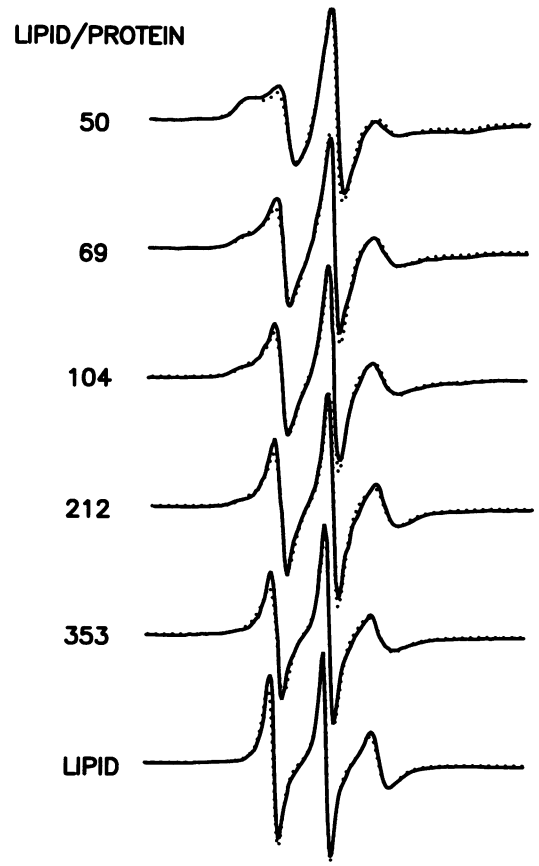

FIGURE 17 Experimental and simulated spectra of 14-PC in DMPC/yeast cytochrome oxidase mixtures at 30°C. ——, experimental spectra digitized from Knowles et al. (1979); ·····, simulations.

TABLE 12 Parameters of components for the simulation of ESR spectra of 14-PC in yeast cytochrome oxidase and DMPC complexes*

C	$R_\perp$ ($\times 10^8$ s^{-1})	$R_\parallel$ ($\times 10^8$ s^{-1})	ϵ_0^2	ϵ_2^2	S
1	0.9	5.0	3.4	1.4	0.82
2	1.5	3.0	2.0	0.7	0.58
3	1.7	2.7	1.2	0.3	0.35
4	1.8	2.5	0.7	0.1	0.15
0†	1.8	2.5	0.5	0.1	0.11

* The ESR spectra of 14-PC in yeast cytochrome oxidase/DMPC complex were digitized from Knowles et al. (1979).
† Component 0 is the simulation for the experimental spectrum from pure DMPC.

We note that ESR spectra similar to those observed from the spin-labeled lipids in DPPC/GA and DMPC/yeast cytochrome oxidase complexes have been reported for a DPPC/Ca^{2+} ATPase reconstituted system (Hesketh et al., 1976), rhodopsin/lipid associations in bovine rod outer segment membranes (Watts et al., 1979), cell membrane vesicles from *H. cutirubrum* (Esser and Lanyi, 1973), and bacteriophage M13 coat protein/lipid reconstructions (Wolfs et al., 1989). Given the similarity between the ESR spectra from these systems, the simulation methods utilized in this study would be applicable to these systems, and we would expect similar

TABLE 13 Populations of the components for the simulation of ESR spectra of 14-PC in yeast cytochrome oxidase/DMPC complexes and average order parameters

L/P*	Component no. 1	2	3	4	$\bar{S}$
50	0.48	0.24	0.16	0.12	0.61
69	0.25	0.25	0.25	0.25	0.48
104	0.18	0.22	0.26	0.34	0.42
212	0.06	0.18	0.27	0.49	0.32
353	0.04	0.07	0.35	0.54	0.28

* L/P = molar ratio of DMPC to yeast cytochrome oxidase.

conclusions from such studies. In fact, for the DMPC/bacteriorhodopsin system, studied by time-resolved fluorescence depolarization, Rehovek et al. (1985) reported a linear increase in order parameter of the DMPC from 0.29 for the pure lipid to 0.62 for a DMPC/bacteriorhodopsin ratio of 52. However, in view of the well-known complexity and specificity of interactions for particular lipid/protein systems (Devaux and Seignenret, 1985), it would be premature to claim that this is the only way the ordering of lipid is affected by membrane proteins. For example, it is observed from an FTIR study that Ca^{2+} ATPase increases the ordering of dioleoylphosphatidylcholine lipid bilayers slightly but decreases the ordering of 1-steroyl-2-oleoylphophatidylcholine bilayers (Mendelsohn and Mantsch, 1986).

CONCLUSIONS

For more than a decade the controversy in interpreting effects of lipid-protein interactions, when the results are obtained from different techniques having different time scales, such as NMR versus ESR, has been puzzling. The conclusions from this study may provide an answer to this classic problem. Our conclusions from the simulation of ESR spectra from DPPC/GA multilamellar vesicles are basically consistent with that from other spectroscopic techniques, such as ^{2}H NMR, FTIR, and Raman. At the same time they are consistent with previous interpretations of the ESR spectra as arising from two or more components when peptide (or protein) is added to the membrane. The principal difference between our conclusions based on detailed simulations and the previous ESR studies, which did not utilize simulations, is that very good agreement with experiment is achieved with a model in which the amplitude of the reorientational motion is restricted (i.e., increased ordering), whereas significantly less satisfactory agreement is achieved with the previously accepted model of sharply decreased motional rates (i.e., immobilized boundary lipid).

The evidence supporting the conclusion that the main effect of GA on the DPPC bilayers is to increase the local ordering is most evident from the 16-PC spectra, since the effect is most dramatic for the terminal region of the acyl chain. The average order parameter of 16-PC increases from 0.06 in the pure lipid to 0.66 for a DPPC/GA ratio of 1. The

GA introduces a significant heterogeneity into the bilayer, as evidenced by the increase in the number of spectral components required to simulate the spectra as the [GA] is increased, an effect most notable for the terminal region of the acyl chain.

The 5-PC and 10-PC spectra provide evidence for the existence of chain structures in which the magnetic tensor axes of the nitroxide are tilted 34° relative to the main chain axes, suggesting the presence of kink structures. The fractional component of such structures initially decreases with [GA], corresponding to a chain ordering effect, but increases with [GA] at the highest [GA]. Our ESR results provide evidence of enhanced water penetration for high [GA], which could be correlated with this "kink disorder" effect.

Incorporation of GA into DPPC bilayers has only a slight effect on the rotational diffusion rates. Generally speaking, the rotation of the acyl chain around the axis parallel to its long molecular axis either is not affected or increases slightly, whereas rotation around the axis perpendicular to its long molecular axis decreases slightly.

While the simulations could, in principle, be improved by allowing for dynamic exchange between the different components, the limited resolution of the MOMD-ESR spectra may not justify the use of the more elaborate models. However, we do note that the detailed interpretation of the 5-PC and 10-PC spectra depends heavily on our choice of model in terms of a superposition of structures with and without kinks, even in the absence of GA.

The similarity of our results for the GA/DPPC system to those for the cytochrome oxidase/DMPC system suggests that there are similar structural effects on the organization of membranes resulting from the incorporation of macromolecules into the bilayer, a matter that could be distinct from any specificity of binding of particular lipids to proteins.

We find that, despite the somewhat limited resolution of the ESR spectra, there are distinct features observed in the experimental spectra that clearly require a multicomponent model. Our conclusions are based on (*a*) the ability to simulate all these features quite accurately; (*b*) having performed very extensive simulations over a wide range of parameters (more than 1000 spectral simulations per labeled lipid and temperature); (*c*) the successful simulation of all spectra from a particular labeled lipid at a given temperature over all ratios of GA/DPPC with the same small subset of component spectra, wherein only their relative populations are varied.

Finally, we do wish to comment that it would be very desirable for future studies if the limited resolution of the MOMD-ESR spectra could be enhanced. This could further improve the reliability of their interpretation. One may hope to achieve enhanced resolution by modern time domain ESR techniques such as two-dimensional ESR (Gorcester et al., 1989; Freed, 1990) and by multifrequency studies, especially at very high frequency (Budil et al., 1989; Freed, 1990). Preliminary results with such techniques on lipid membrane vesicles in this laboratory are encouraging in this respect.

We wish to thank Drs. David Budil and Jozef Moscicki for helpful discussions and a critical reading of the manuscript. This work was supported by National Institutes of Health grant GM25862. Computations were performed at the Cornell National Supercomputer Facility.

REFERENCES

Bienvenue, A., M. Bloom, J. H. Davis, and P. F. Devaux. 1982. Evidence for protein-associated lipids from deuterium nuclear magnetic resonance studies of rhodopsin dimyristoylphosphatidylcholine recombinants. *J. Biol. Chem.* 257:3032–3038.

Boyer, R. F. 1966. Introductory remarks for symposium on transitions and relaxations in polymers. *J. Polym. Sci., Part C.* 14:3–14.

Budil, D. E., K. E. Earle, W. B. Lynch, and J. H. Freed. 1989. Electron paramagnetic resonance at 1 millimeter wavelengths. *In* Advanced EPR: Applications in Biology and Biochemistry. A. J. Hoff, editor. Elsevier, Amsterdam. 307–340.

Casal, H. L., and R. N. McElhancy. 1990. Quantitative determination of hydrocarbon chain conformational order in bilayers of saturated phosphatidylcholines of various chain lengths by Fourier transform infrared spctroscopy. *Biochemistry.* 29:5423–5427.

Chapman, D., B. A. Cornell, A. W. Eliasz, and A. Perry. 1977. Interactions of helical peptide segments which span the hydrocarbon region of lipid bilayers. Studies of the gramicidin A lipid-water system. *J. Mol. Biol.* 113:517–538.

Cornell, B. A., M. M. Sacre, W. E. Peel, and D. Chapman. 1978. The modulation of lipid bilayers fluidity by intrinsic polypeptides and proteins. *FEBS Lett.* 90:29–35.

Cornell, B. A., L. E. Wier, and F. Separovic. 1988. The effect of gramicidin A on phospholipid bilayers. *Eur. Biopys. J.* 16:113–119.

Cortijo, M., A. Alonso, J. C. Gomez-Fernandez, and D. Chapman. 1982. Intrinsic protein-lipid interactions: infrared spectroscopic studies of gramicidin A, bacteriorhodopin and Ca^{2+}-ATPase in biomembranes and reconstituted systems. *J. Mol. Biol.* 157:597–618.

Crepeau, R. H., S. Rananavare, and J. H. Freed. 1987. Automated least-squares fitting of slow motional ESR spectra. Abstracts of the 10th International ESR Symposium, Rocky Mountain Conference, Denver, CO, August 1987.

Dahlquist, F. W., D. C. Muchmore, J. H. Davis, and M. Bloom. 1977. Deuterium magnetic resonance studies of the interaction of lipids with membrane proteins. *J. Proc. Natl. Acad. Sci. USA.* 74:5435–5439.

Devaux, P. F., and M. Seignenret 1985. Specificity of lipid-protein interactions as determined by spectroscopic techniques. *Biochim. Biophys. Acta.* 822:63–125.

Esser, A. F., and J. K. Lanyi. 1973. Structure of the lipid phase in cell envelope vesicles from *Halobacterium cutirubrum. Biochemistry.* 12:1933–1939.

Ferrarini, A., P. L. Nordio, G. L. Moro, R. H. Crepeau, and J. H. Freed. 1989. A theoretical model of phospholipid dynamics in membranes. *J. Chem. Phys.* 91:5707–5721.

Flory, P. J. 1989. Statistical Mechanics of Chain Molecules. Hanser Publishers, Munich.

Freed, J. H. 1990. The Bruker lecture: modern techniques in EPR spectroscopy. *J. Chem. Soc. Faraday Trans.* 86:3173–3180.

Gorcester, J., G. L. Millhauser, and J. H. Freed. 1989. Two dimensional and Fourier transform EPR. *In* Advanced EPR: Applications in Biology and Biochemistry. A. J. Hoff, editor. Elsevier, Amsterdam. 177–242.

Griffith, O. H., P. J. Dehlinger, and S. P. Van. 1974. Shape of the hydrophobic barrier of phospholipid bilayers (evidence for water penetration in biological membranes). *J. Membr. Biol.* 15:159–192.

Hesketh, T. R., G. A. Smith, M. D. Houslay, K. A. McGill, and N. J. M. Birdsall. 1976. Annular lipid determine the ATP-ase activity of a calcium transport protein. *Biochemistry.* 15:4145–4151.

Ho, C., and C. D. Stubbs. 1992. Hydration at the membrane protein-lipid interface. *Biophys. J.* 63:897–902.

Jost, P. C., and O. H. Griffith, editors. 1982. Lipid-Protein Interactions. Vol. 2. John Wiley and Sons, New York.

Jost, P. C., O. H. Griffith, R. A. Capaldi, and G. A. Vanderkooi. 1973. Evidence for boundary lipid in membranes. *J. Proc. Natl. Acad. Sci. USA.* 70:480–484.

Kang, S. Y., H. S. Gutowsky, J. C. Hsung, R. Jacobs, T. E. King and D. Rice. 1979. Nuclear magnetic resonance investigation: a new model for boundary lipid. *Biochemistry.* 18:3257–3267.

Kar, L., E. Ney-Igner, and J. H. Freed. 1985. Electron spin resonance and electron-spin-echo study of oriented multilayers of L_α-dipalmitoylphosphatidylcholine water system. *Biophys. J.* 48:569–595.

Killian, J. A. 1992. Gramicidin and gramicidin-lipid interactions. *Biochim. Biophys. Acta.* 1113:391–425.

Kinosita, K., Jr., A. Ikegami, and S. Kawato. 1981. The effect of cytochrome oxidase on lipid chain dynamics. A nanosecond fluorescence depolarization study. *Biochim. Biophys. Acta.* 647:7–17.

Knowles, P. F., A. Watts, and D. Marsh. 1979. Spin-labeled studies of lipid immobilization in dimyristoylphosphatidylcholine-substituted cytochrome oxidase. *Biochemistry.* 18:4480–4487.

Langs, D. A., and D. J. Triggle. 1992. Structural motifs for ion channels in membranes. *In* The Structure of Biological Membranes. P. Yeagle, editor. CRC Press, Boca Raton, FL. 721–780.

Lee, D. C., A. A. Durrani, and D. Chapman. 1984. A difference infrared spectroscopic study of gramicidin a, alamethicin and bacteriorhodopsin in perdeuterated dimyristoylphosphatidylcholine. *Biochim. Biophys. Acta.* 769:49–56.

Longmuir, K. J., R. A. Capaldi, and F. W. Dahlquist. 1977. Nuclear magnetic resonance studies of lipid-protein interactions. A model of the dynamics and energetics of phosphatidylcholine bilayers that contain cytochrome *c* oxidase. *Biochemistry.* 16:5749–5755.

Marsh, D. 1989. Experimental methods in spin-label spectral analysis. *In* Biological Magnetic Resonance. Vol. 8. L. J. Berliner and J. Reuben, editors. Plenum Press, New York. 255–303.

Marsh, D., and A. Watts. 1982. Spin labeling and lipid-protein interactions in membranes. *In* Lipid-Protein Interactions. P. C. Jost and O. H. Griffith, editors. John Wiley and Sons, New York. 53–126.

Meirovitch, E., A. Nayeem, and J. H. Freed. 1984. Analysis of protein-lipid interactions based on model simulations of electron spin resonance spectra. *J. Phys. Chem.* 88:3454–3465.

Mendelsohn, R., and H. H. Mantsch. 1986. Fourier transform infrared studies of lipid-protein interactions. *In* Progress in Protein-Lipid Interactions. Vol. 2. A. Watts and J. J. H. H. M. De Pont, editors. Elsevier, Amsterdam. 103–146.

Mendelsohn, R., R. Dluhy, T. Taraschi, D. G. Cameron, and H. H. Mantsch. 1981. Raman and Fourier transform infrared spectrocopic studies of the interaction between glycophin and dimyristoylphosphatidylcholine. *Biochemistry.* 20:6699–6706.

Mendelsohn, R., M. A. Davis, J. W. Brauner, H. F. Schuster, and R. A. Dluhy. 1989. Quantitative determination of conformational disorder in the acyl chains of phospholipid bilayers by infared spectroscopy. *Biochemistry.* 28:8934–8949.

Mouritsen, O. G. 1986. Physics of biological membranes. *In* Physics in Living Matter. D. Baeriswyl, M. Droz, A. Malaspinas, and P. Martinoli, editors. Springer-Verlag, Berlin. 76–109.

Owicki, J. C., and H. M. McConnell. 1979. Theory of protein-lipid and protein-protein interactions in bilayer membranes. *J. Proc. Natl. Acad. Sci. USA.* 76:4750–4754.

Owicki, J. C., M. W. Springgate, and H. M. McConnell. 1978. Theoretical study of protein-lipid interactions in bilayer membranes. *J. Proc. Natl. Acad. Sci. USA.* 75:1616–1619.

Paddy, M. F., F. W. Dahlquist, J. H. Davis, and M. Bloom. 1981. Dynamical and temperature-dependent effects of lipid-protein interactions. Application of deuterium nuclear magnetic resonance and electron paramagnetic resonance spectroscopy to the same reconstitutions of cytochrome *c* oxidase. *Biochemistry.* 20:3152–3162.

Peterson, N. O., and S. I. Chan. 1977. More on the motional state of lipid bilayer membranes: interpretation of order parameters obtained from nuclear magnetic resonance experiments. *Biochemistry.* 16:2657–2667.

Rajan, S., S. Y. Kang, H. S. Gutowsky, and E. Oldfield. 1981. Phosphorus nuclear magnetic resonance study of membrane structure. *J. Biol. Chem.* 256:1160–1166.

Rehovek, M., N. A. Dencher, and M. P. Heyn. 1985. Long-range lipid-protein interactions. Evidence from time-resolved fluorescence depolarization and energy-transfer experiments with bacteriorhodopsin-dimyristoylphosphatidylcholine vesicles. *Biochemistry.* 24:5980–5988.

Rice, D., and E. Oldfield. 1979. Deuterium nuclear magnetic resonance studies of the interaction between dimyristoylphosphatidylcholine and gramicidin A. *Biochemistry.* 18:3272–3279.

Schneider, D. J., and J. H. Freed. 1989. Calculating Slow Motional Magnetic Resonance Spectra: A User's Guide. *In* Biological Magnetic Resonance. Vol. 8. L. J. Berliner and J. Reuben, editors. Plenum Press, New York. 1–76.

Seelig, A., and J. Seelig. 1974. The dynamic structure of fatty acyl chains in a phospholipid bilayer measured by deuterium magnetic resonance. *Biochemistry.* 13:4839–4845.

Seelig, J., and A. Seelig. 1980. Lipid conformation in model membranes and biological membranes. *Q. Rev. Biophys.* 13:19–61.

Seelig, J., N. Seelig, and Tamm, L. 1982. Nuclear magnetic resonance and lipid-protein interactions. *In* Lipid-Protein Interactions. Vol. 2. P. C. Jost and O. H. Griffith, editors. John Wiley and Sons, New York. 127–148.

Selinsky, B. S. 1992. Protein-lipid interactions and membrane function. *In* The Structure of Biological Membranes. P. Yeagle, editor. CRC Press, Boca Raton, FL. 573–601.

Sheater, H. M. M., and V. Vand. 1956. The crystal structure of the monoclinic form of *n*-hexatriacontane. *Acta Cryst.* 9:379–384.

Shin, Y-K., and J. H. Freed. 1989. Thermodynamics of phosphatidylcholine-cholesterol mixed model membranes in the liquid crystalline state studied by the orientational order parameter. *Biophys. J.* 56:1093–1100.

Sholnick, J., and E. Helfand 1980. Kinetics of conformational transitions in chain molecules. *J. Chem. Phys.* 77:5489.

Short, K. W., B. A. Wallace, R. A. Myers, S. P. A. Fodor, and A. K. Dunker. 1987. Comparison of lipid/gramicidin dispersions and cocrystals by Raman scattering. *Biochemistry.* 26:557–562.

Tanaka, H., and J. H. Freed. 1985. Electron spin resonance studies of lipid-gramicidin interactions utilizing oriented multibilayers. *J. Phys. Chem.* 89:350–360.

Urry, D. W. 1971. The gramicidin A transmembrane channel: a proposed $\Pi_{(L,D)}$ helix. *J. Proc. Natl. Acad. Sci. USA.* 68:672–676.

Urry, D. W. 1972. A molecular theory of ion-conducting channels: a field dependent transformation between conducting and nonconducting conformations. *J. Proc. Natl. Acad. Sci. USA.* 69:1610–1614.

Watts, A., and J. J. H. H. H. De Pont, editors. 1986. Progress in Protein-Lipid Interactions. Vols. 1–2. Elsevier, Amsterdam.

Watts, A., I. D. Volotovski, and D. Marsh. 1979. Rhodopsin-lipid associations in bovine rod outer segment membranes. Identification of immobilized lipid by spin-labels. *Biochemistry.* 18:5006–5013.

Williams, B. W., and C. D. Stubbs. 1988. Properties influencing fluorophore lifetime distributions in lipid bilayers. *Biochemistry.* 27:7994–7999.

Williams, B. W., A. W. Scotto, and C. D. Stubbs. 1990. Effect of proteins on fluorophore lifetime heterogeneity in lipid bilayers. *Biochemistry.* 29: 3248–3255.

Wolfs, C. J. A., L. I. Horvath, D. Marsh, A. Watts, and M. A. Hemminga. 1989. Spin-label ESR of bacteriophage M13 coat protein in lipid bilayers. Characterization of molecular selectivity of charged phospholipids for the bacteriophage M13 coat protein in lipid bilayers. *Biochemistry.* 28: 9995–10001.